







ARTICLE (Non-peer reviewed preprint) 2

Harmonizing past and future global sectoral water use data

 3Ioan Sabin Taranu ^{*,1} Inne Vanderkelen ^{2,3} Yoshihide Wada ⁴ Ting Tang ⁴ Steven Eisenreich ⁴ and Ann Van Griensven ¹ 4

5

¹Vrije Universiteit Brussels, Department of Water and Climate, Brussels, Belgium. 6²Department of Earth and Environmental Sciences, KU Leuven, Leuven, Belgium. 7³Royal Meteorological Institute of Belgium, Brussels, Belgium. 8⁴Biological and Environmental Science and Engineering Division, King Abdullah University of Science and Technology, Thuwal, Saudi Arabia. 9

10

*Corresponding author: Sabin.Taranu@vub.be 11

Abstract

The use of water in the domestic, agricultural, and industrial sectors is necessary for human prosperity and survival. Recognizing the need to understand water scarcity and human contributions to it, various studies have been done over the years, necessitating access to reliable, comprehensive data on historical and projected water use across all sectors. Despite progress in this direction, a significant challenge persists in finding datasets that maintain consistency at both national and subnational levels at the intersection between historical and future projections. This inconsistency is likely attributed to factors such as discordant socio-economical data at the transition between historical and future periods (e.g., GDP, population dynamics, livestock density, land use) and the independent creation of past and scenario datasets without concerted efforts for harmonization. Addressing these issues, this study presents a first holistic approach to harmonize two existing water use datasets across all sectors, encompassing both past and projected periods. The methodology and insights gained from this process are discussed, highlighting the achievement of a fully consistent dataset. The harmonized dataset offers utility for a broad spectrum of applications at the interface between humans, water, and climate.

Keywords: sectoral water use; data harmonization; 12

12

1. Introduction

 13

13

Water is fundamental to sustaining life and facilitating human prosperity, serving a multitude of applications that range from domestic needs, such as drinking, sanitation, and cooking, to agricultural, industrial, and environmental functions. These include livestock water needs, electricity production through cooling power plants, manufacturing of various goods, mining, irrigation, and maintaining environmental flow requirements. As such, efficient management and utilization of water resources are essential to ensure human health and the continued development of societies around the world. 14

14

15

16

17

18

19

However, the stark reality is that more than 4 billion people are currently grappling with water scarcity [1], a crisis driven by a complex interplay of factors. These factors include limited water availability in certain regions [2], increased demands fueled by population growth, urbanization, and higher standards of living [3], inefficient water usage and management practices, inadequate infrastructure, water pollution [4, 5], and significant changes in the hydrological cycle due to changes in land use [6] and excessive extraction of water resources beyond their renewable capacity [7, 8]. Moreover, the advent of climate change introduces additional complexities, manifested in increased evapotranspiration, altered precipitation patterns, and more frequent and severe hot and dry extremes [9, 10, 11, 12, 13, 14]. These changes are expected to exacerbate the already challenging task 20

20

21

22

23

24

25

26

27

28

of ensuring the water supply worldwide.

The modern understanding of the global human-water-climate dynamics is significantly relying on the use of Global Hydrological and Earth System Models (GHMs and ESMS respectively) [14]. These models are equipped to accurately represent the entire water cycle, capturing the dynamics of water balance in various bodies of water and encompassing essential processes such as runoff, evapotranspiration, changes in snow cover and infiltration. These models also integrate human-related water management practices, including reservoir operations [15, 16], water abstractions [17, 18, 19, 20, 21, 22], pollution [23, 24], and the exploration of alternative water sources such as desalination and wastewater reuse [25, 4].

Based on GHM/ESM simulations, we are able to expand our understanding of topics related to water scarcity and available adaptation options. Some notable applications include understanding the role of human impacts in generating water scarcity [26, 27], the balance between environmental and human needs [28], national and regional evaluations of water availability and stress [29, 30], future sustainability in various scenarios [31], or analysis of feasibility and impact of different adaptation measures [32, 33, 34]. It was also shown that considering human-related impacts, including land use change, reservoir operations and water abstractions results in a general performance increase of GHMs to represent streamflow and hydrological extremes [35].

In this context, the importance of accurately representing human-related forcings in the water cycle becomes apparent. More specifically, this study emphasizes the need for reliable sectoral data on water use. Although previous research has indicated potential discrepancies between modeled sectoral water use and actual national or sub-national patterns [36], our focus is on the consistency of this data across spatial and temporal scales, particularly between historical and future projections. A key challenge identified is the mismatch in time-series data at the national and gridcell levels, often manifesting as abrupt shifts at the transition points between past and future periods. This issue primarily arises from the reliance on predictors such as GDP, population density, and land use changes, which may be inconsistent at the historical to future transition (see Appendix), as well as the independent creation of past and projections datasets without harmonization efforts.

Given that sectoral water use data play an important role in GHMs/ESMs and subsequent analyzes, such spatial and temporal inconsistencies could significantly affect the validity of assessments derived from these models. The abrupt changes in national and sub-national water use statistics potentially compromise the reliability of indices that evaluate historical versus future periods, possibly obscuring or generating misleading signals.

To address these critical gaps, this article has two primary objectives: (i) to propose a harmonization strategy for the existing generation of water use datasets to enhance their utility for research and modeling applications, and (ii) to discuss potential solutions to prevent these discrepancies in future datasets. By directly addressing these challenges, this study aims to contribute to the field of water management and sustainability, providing actionable insights to researchers, modelers, and stakeholders involved in global efforts to alleviate water scarcity.

2. Methods

2.1 Historical water use data

Historical data on sectoral withdrawal and consumption is sourced from Huang et al. (2018) [37] (Table 1). This dataset represents a historical reconstruction, which is generated by combining the US Geological Survey (USGS) and the Liu et al. (2016) [38] improved Food and Agriculture Organization of the United Nations (FAO) AQUASTAT dataset on sectoral water use. It covers the period 1971–2010, and it is available on a regular $0.5 \times 0.5^\circ$ grid and monthly frequency. The represented

sectors are domestic, livestock, thermoelectric, manufacturing, mining, and irrigation. 74

To obtain the final monthly gridded dataset, Huang et al. (2018) used a three-step approach, involving 75
 spatially downscaling the original country (or state) level data to the $0.5 \times 0.5^\circ$ grid level, followed by 76
 linear interpolation on the individual grid cells' time-series to get annual sectoral withdrawal from 77
 the 5-year interval from reports, and ultimately, using a sector-dependent temporal downscaling 78
 procedure to go from annual to monthly frequency. The only exception is the irrigation sector, 79
 for which a combination of model simulations and national reported values was used. In this case, 80
 the simulated irrigation withdrawals of 4 GHMs (WaterGAP, LPJmL, H08, and PCR-GLOBWB) for 81
 the historical period were scaled using available national reported statistics, while maintaining the 82
 original GHMs subnational patterns of irrigation abstractions [37]. Instead of using the 4 original 83
 irrigation withdrawal datasets, we calculated their ensemble mean, and used it as the target for the 84
 harmonization. Although originally the dataset contains also sectoral consumption, in this study we 85
 make use only of the withdrawal data. 86

For spatial downscaling, Huang et al. (2018) used global population density maps from the History 87
 Database of the Global Environment (HYDE; 1970-1980) and Gridded Population of the World (GPW; 88
 1990-2010) for the domestic, thermoelectric, manufacturing, and mining sectors, while using 2005 89
 FAO global livestock density maps for the livestock sector, following the approach of Hejazi et al. 90
 (2014) [39]. A uniform distribution is adopted for the temporal downscaling of water withdrawal of 91
 livestock, mining, and manufacturing. For the domestic sector, a temporal downscaling based on the 92
 approach of Wada et al. (2011) [40] is used, where a modulating function is applied based on each 93
 grid cell's historical temperature ranges and a region-dependent amplitude parameter R [37]. Finally, 94
 thermoelectric water withdrawal is temporally downscaled using the assumption that thermoelectric 95
 water use is proportional to generated electricity, which is then estimated using heating degree-days 96
 (HDD) and cooling degree-days (CDD) as proxies [41, 42]. The temporal downscaling algorithms, 97
 for both the domestic and the thermoelectric sectors, were validated and calibrated based on existing 98
 observations [37]. 99

The main reason why we selected this dataset to represent the historical period is because it was 100
 primarily derived from existing observation/reported data, and its separation of the industrial sector 101
 in manufacturing, thermoelectric, and mining sectors offers more research opportunities as each 102
 sector have their own role and socio-economic value provided [43]. 103

2.2 Future water use data 104

Future data on sectoral water use was sourced from Khan et al., 2023 [44] (Table 1). This dataset 105
 represents a large collection of future water use scenarios. In total, 75 possible scenarios are pro- 106
 vided, consisting of a combination of 4 Representative Concentration Pathways (RCPs) [45], 5 Shared 107
 Socioeconomic Pathways (SSPs) [46], and 5 Global Climate Models (GCMs) from the Inter-sectoral 108
 Impact Model Intercomparison Project (ISIMIP) protocol 2b [47]. Sectoral withdrawal and consump- 109
 tion data are available on a global $0.5 \times 0.5^\circ$ grid, at a monthly frequency, and cover the period 2010 to 110
 2100. To generate the data, the authors combined the Global Change Analysis Model (GCAM) with 111
 a spatial downscaling model of land use (Demeter), a global hydrological framework (Xanthos) and 112
 a downscaling package (Tethys) [48, 44]. In this study, we present the results for a subset of eight 113
 scenarios, as described in Table 1 to showcase the added value of the harmonization process. 114

This dataset was selected for the future period, because it covers the same sectors as the historical 115
 reconstruction of Huang et al. 2018 [37, 44]. In addition, there are significant similarities in the spatial 116
 and temporal downscaling approaches between the two studies. In particular, both studies have 117
 identical temporal downscaling approaches for all sectors except irrigation [37, 44]. For irrigation, 118
 Huang et al. 2018 provides 4 different reconstructions of historical irrigation abstractions based on 119

Table 1. Water use data used in this study.

Source	Water Use Types	Sectors	Spatial Scope	Temporal Scope	Scenarios
Huang et al., 2018	- Withdrawals	- Domestic - Livestock - Electric - Manufacturing - Mining - Irrigation (ensemble mean of the 4 available models)	- Global - 0.5deg gridded	- 1971-2010 - Monthly	Historical
Khan et al., 2023	- Withdrawals	- Domestic - Livestock - Electric - Manufacturing - Mining - Irrigation	- Global - 0.5deg gridded	- 2010-2100 - Monthly	Future - SSP2 - RCP2.6, RCP6.0 - 4 CMIP5 GCMs (GFDL, HADGEM, IPSL, MIROC)

the method described earlier (Sect. 2.1), which leads to each reconstruction maintaining the monthly weights representative of the corresponding GHMs. Although we calculated the ensemble mean for these four models, it is likely that the temporal weights still differ significantly. For example, the temporal downscaling of future irrigation abstractions uses the monthly weights of a single model (PCR-GLOBWB), averaged over the period 1971–2010 [44].

For spatial downscaling of non-agricultural sectors (domestic, electricity, manufacturing, and mining), both studies use the same underlying population map to downscale water use [37, 44]. In the case of livestock, the spatial downscaling is based on the same version of the 2005 livestock density map [49], but the studies apply different methods to account for individual livestock types [50, 37, 44]. Finally, the spatial downscaling for irrigation differs considerably between the two datasets. In the historical dataset, the four irrigation reconstructions preserve the spatial structure of the original GHMs (Section 2.1), although in our case, this structure is modified by calculating the mean of the ensemble. In contrast, in the future dataset, irrigation downscaling is performed using the spatial breakdown provided by Demeter, a high-resolution downscaling model that uses GCAM output to calculate global gridded land-use change [51, 44].

2.3 National level time-series continuity

When analyzing historical national statistics for socioeconomic variables such as population, GDP, or sectoral water use, significant fluctuations and discontinuities are not uncommon. These variations can be attributed to factors such as economic booms or crashes, population displacement or loss due to war, or changes in data collection and reporting methods. In contrast, future projections typically exhibit smoother trends, with potential shifts occurring over time, but without the abrupt changes seen in historical data.

When conducting national assessments, one critical criterion for socioeconomic data is the continuity of the time-series at the transition between historical and future periods. This continuity is essential for accurately analyzing temporal trends in both relative and absolute terms. However, achieving continuous time-series for all countries globally, especially in complex models such as those used in sectoral water use data (see Sections 2.1-2.2), presents a significant challenge.

An approach to ensure continuity is to generate both historical and future data through a single continuous simulation that spans both periods. However, this strategy requires that the predictor inputs are also continuous. The drawback of this approach is that even with optimal model tuning, the historical outputs may not fully align with documented statistics. If strict alignment with historical data is required, a bias-correction of the historical results may be necessary. Although

this is feasible, it may not yield the best results, as documented statistics often contain significant fluctuations and discontinuities that would be difficult to replicate in a global model. Therefore, this approach is most suitable when historical data are sparse or unreliable.

The second approach, and the one applied in this study, is to combine documented statistics for the historical period and future projections based on available models. In this case, the primary focus is on the quality of future scenarios and the trends they reflect. However, this method may result in discontinuities at the transition between historical and projected periods. To address this, a harmonization procedure is necessary to ensure continuity.

In this study, we aggregate sectoral water use data at the national level (or at the state level for the U.S.) for each sector and verify the continuity of the time-series at the transition between historical and projected periods. A harmonization procedure is then applied, tailored to the specific properties of each sector and dataset.

2.4 Spatial consistency

Beyond the national scale, one could argue that maintaining time-series continuity should also extend to grid cell levels, at least in certain cases. The rationale for this is similar to the need for continuity at the national level.

For example, in the case of sectoral water use, the key predictors for projections or spatial downscaling include socioeconomic data such as population density, livestock density, thermoelectric power plant locations, land use patterns, nighttime lights, and more. Although for the historical period, it is more common to consider within-country population displacements (e.g., due to floods), the construction of reservoirs or thermoelectric plants at certain moments in time, and other events that can introduce fluctuations at the gridcell level, such time-discrete features are less frequently incorporated into future scenarios.

Given this, we would expect that any fluctuations in gridcell time-series during the transition year would generally be consistent with those observed in subsequent years. If this is not the case and a significant change occurs at the transition, this could indicate spatial inconsistencies within the dataset. These inconsistencies may stem from uncoordinated or inconsistent predictor data (e.g., a high population concentration in one grid during the historical period that shifts to a neighboring grid in the future predictor dataset, see Appendix) or from differences in downscaling methodologies.

However, if pronounced spatial inconsistencies are detected, they should be addressed. This is particularly important because research often presents results at the gridcell level using gridded maps or computes indices at this level before aggregating them to larger scales. Systematic spatial inconsistencies in the datasets could lead to artificial dampening or amplification of signals when comparing historical and future states.

2.5 Harmonization algorithm

2.5.1 Define the main issues

To design the harmonization algorithm, it is important to first understand the types of issues that can arise in the data we intend to use. By analyzing the continuity of national-level time series (Fig. 1), we identified two primary issues:

- Discontinuities in mean annual values at the transition year.
- Abrupt changes in seasonality at the transition year, characterized by sudden increases or decreases in amplitude. Here, we define seasonality as the difference between the minimum and maximum values recorded within a given year.

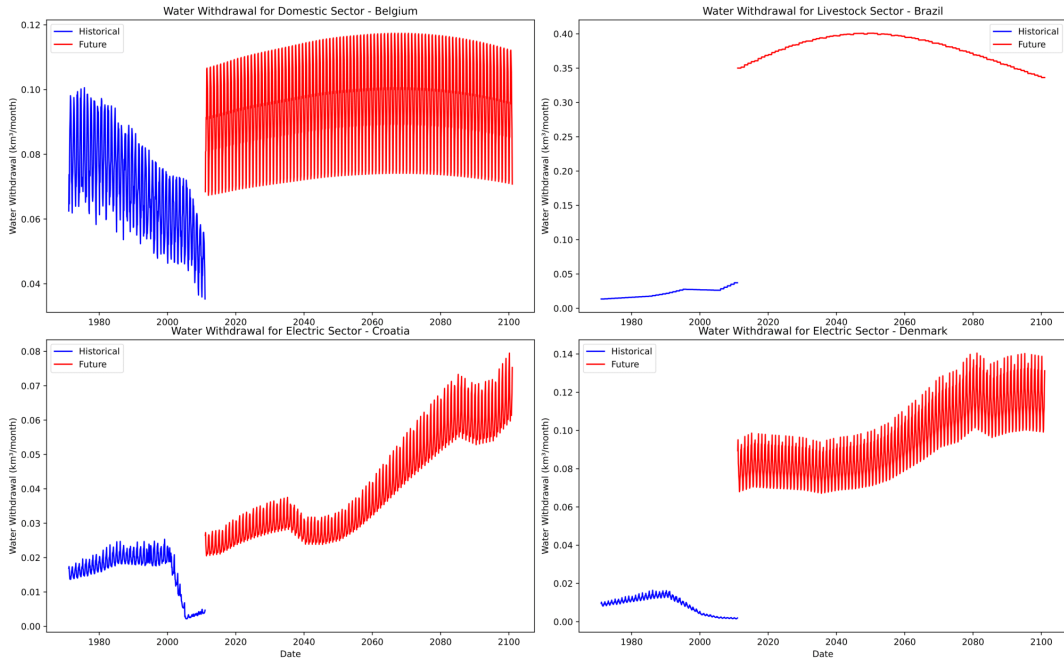


Figure 1. Original domestic withdrawal time-series aggregated at national level. For this example, future data is based on the SSP2-RCP2.6-GFDL scenario.

From a spatial perspective, we examined the relative change in sectoral water withdrawal between consecutive years (Fig. 2). This analysis revealed that many regions experience a sudden drop or a spike at the transition year (2010–2011). Based on this figure alone, it is difficult to determine whether these changes are solely due to the misalignment of national time-series or if differences in the downscaling techniques also contribute. This issue will be explored in greater detail in the Results and Discussion sections.

2.5.2 Outline the requirements for the algorithm

Considering the identified issues and the diverse range of sectors and their specific characteristics, we need to develop a harmonization algorithm with the following capabilities:

- A simple bias adjustment to correct misalignment in mean values, effectively shifting the future time-series up or down as needed.
- In some cases (though not shown here), applying bias adjustments may result in negative values in the future national time-series. The harmonization algorithm should address such instances while preserving the overall trend in future sectoral water abstraction data as much as possible.
- Adjustment of seasonality amplitude to ensure smooth continuity at the transition year. It is important to note that the seasonality in future projections is not static and may vary from year to year. Therefore, the solution must preserve future trends in seasonality changes while ensuring the amplitude matches at the transition year.
- For most sectors, seasonality amplitude and mean values in historical time-series change gradually from year to year. However, this is not always true for the irrigation sector, where in a particularly wet year, irrigation withdrawals may approach zero, only to increase significantly the following year. It is therefore essential to include a feature that accounts for this high interannual variability.

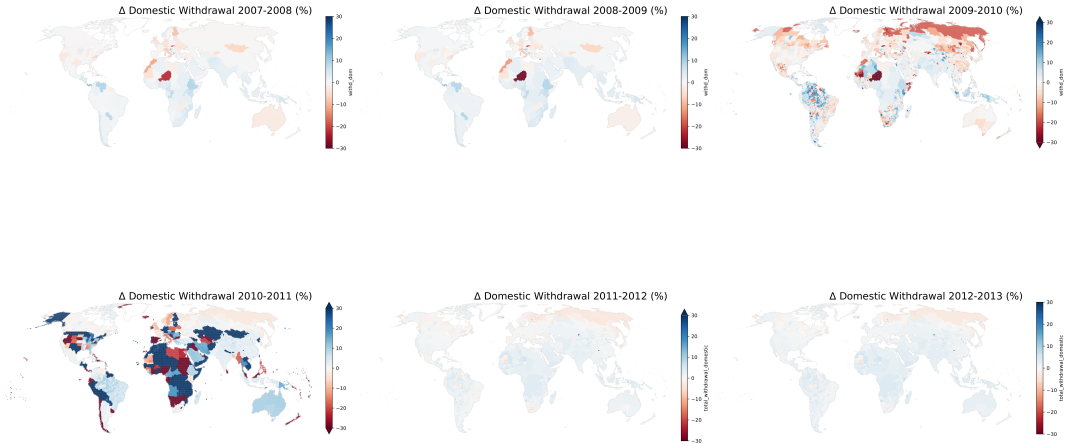


Figure 2. Consecutive years relative change in domestic withdrawal calculated at gridcell level from the original historical and future datasets. The years 2010–2011 represent the transition year between the past and future periods. For this example, future data is based on the SSP2-RCP2.6-GFDL scenario.

- Lastly, spatial inconsistencies at the transition year may arise not only from misalignment in national time-series, but also from the use of different downscaling techniques. For example, the same national data for a given year may be distributed differently across grids depending on the proxy data or methodology used. As these inconsistencies are more challenging to resolve in a general way, we will address them separately on a case-by-case basis, outside the main harmonization algorithm.

2.5.3 Proposed solution

Let $\mathbf{H}(t)$ denote the historical time-series data of a given country or US state, where $t \in [t_0, t_{\text{end}}]$ (equivalent to [1971,2010] in our case), and let $\mathbf{F}(t)$ denote the future time-series data, where $t \in [t_{\text{future}}, t_{\text{max}}]$ (equivalent to [2010,2100] in our case). We seek to apply corrections to $\mathbf{F}(t)$ to ensure consistency with $\mathbf{H}(t)$.

1: Historical Amplitude and Middle Point Calculation

For a given historical period $[t_{\text{start}}, t_{\text{end}}]$, where $N = t_{\text{end}} - t_{\text{start}} + 1$, we calculate the following metrics for each year $t \in [t_{\text{start}}, t_{\text{end}}]$:

- **Yearly Maximum:**

$$\text{Max}_H(t) = \max(\mathbf{H}(t))$$

- **Yearly Minimum:**

$$\text{Min}_H(t) = \min(\mathbf{H}(t))$$

- **Yearly Amplitude:**

$$A_H(t) = \text{Max}_H(t) - \text{Min}_H(t)$$

Next, we compute the average historical amplitude A_H^{avg} over the N years:

$$A_H^{\text{avg}} = \frac{1}{N} \sum_{t=t_{\text{start}}}^{t_{\text{end}}} A_H(t)$$

We also calculate the historical middle point, but only for $t = t_{\text{end}}$ (2010 in this case):

$$M_H^{2010} = \frac{\text{Max}_H(t = 2010) + \text{Min}_H(t = 2010)}{2}$$

For all sectors except irrigation, we use $N=1$, which is equivalent to using only the last historical year (2010) as a reference from which we derive the variable of interest. In the case of irrigation, we found $N=5$, which is equivalent to using the years [2006, 2010], to provide satisfactory results, avoiding the problem where the reference seasonal amplitude would be based on a single, potentially outlier year. For the middle point, we found that using the last historical year is enough.

2: Bias Adjustment

For future data $\mathbf{F}(t)$ and the year that overlaps $t = 2010$, we calculate the future middle point:

$$M_F^{2010} = \frac{\max(\mathbf{F}(t = 2010)) + \min(\mathbf{F}(t = 2010))}{2}$$

We then adjust the future data to correct the bias between the historical and future middle points:

$$\mathbf{F}^{\text{bias}}(t) = \mathbf{F}(t) + (M_H^{2010} - M_F^{2010})$$

where $\mathbf{F}^{\text{bias}}(t)$ represents the bias-adjusted future data.

3: Iterative Rescaling to Correct for Negative Values

To eliminate negative values in the future data, we apply an iterative min-max rescaling process over the entire future time-series. The min-max rescaling is a simple method which allows normalizing a given data within a selected range. The general formula to rescale a range between an arbitrary set of values $[\text{Min}_{\text{new}}, \text{Max}_{\text{new}}]$ is:

$$y' = \text{Min}_{\text{new}} + \frac{y - \text{Min}_{\text{old}}}{\text{Max}_{\text{old}} - \text{Min}_{\text{old}}} \times (\text{Max}_{\text{new}} - \text{Min}_{\text{new}})$$

where y is an original value, y' is the corresponding normalized value, Min_{old} and Max_{old} are the original dataset min and max values, and the Min_{new} and Max_{new} are the new min and max value of the normalized dataset. For the following, we will keep this organization of the formula, so it is easy to recognize how the new min and max values are defined.

Let $\mathbf{F}^{\text{bias, rescaled}}$ be the bias adjusted and negative values corrected data for the entire future period [2010,2100]. We aim to ensure:

$$\min(\mathbf{F}^{\text{bias, rescaled}}(t)) \geq 0$$

If negative values exist, we rescale the data iteratively as follows:

- Define the new minimum as $\min(\mathbf{H}(t))$ scaled by a factor α :

$$\min_F^{\text{new}} = \alpha \cdot \min(\mathbf{H}(t))$$

For example, if $\alpha = 0.1$, then the \min_F^{new} will be equivalent to 10% of the minimum value registered in the entire historical time-series for the given country. This minimum target value will be kept constant throughout the iterative rescaling process.

- Define the new maximum:

$$\max_F^{\text{new}}(i = 0) = \max(\mathbf{F}^{\text{bias}}(t))$$

Compared to the constant minimum target value, the maximum is adjusted as needed in each iteration i . The reason for this is that when we perform the first rescaling, the historical and future time-series might become miss-aligned in terms of middle points, so to achieve alignment, while avoiding negative values and trying to maintain as much as possible the original future trajectory of the time-series, we need to gradually adjust the maximum target till the middle points of historical and future time-series become aligned. We do this in the following way:

$$\max_F^{\text{new}}(i) = \max_F^{\text{new}}(i - 1) \times (1 - 0.25 \times \Delta M(t = 2010, i))$$

Where $\Delta M(t = 2010, i)$ is the relative error in the alignment of the historical and the rescaled future time-series middle points for the overlapping year 2010:

$$\Delta M(t = 2010, i) = \frac{M_F^{\text{bias, rescaled, 2010}}(i) - M_H^{2010}}{M_H^{2010}}$$

By introducing the relative alignment error in the adjustment process for the new maximum computation, we obtain a very soft convergence towards the minimum change of the original maximum so that we maintain as much as possible the original trajectory of the future time-series. Here we should also mention that we introduce a cap in the alignment error adjustment such that:

$$0.005 \leq 1 - 0.25 \times \Delta M(t = 2010, i) \leq 0.25$$

The minimum value (0.5%) is introduced to ensure faster convergence for small missalignments, while we limit the maximum factor (0.25%) to keep the adjustments more conservative even when the missalignments are larger than 100%.

- Finally, we apply the rescaling to the entire future data:

$$\mathbf{F}^{\text{bias, rescaled}}(t, i) = \min_F^{\text{new}} + \frac{\mathbf{F}^{\text{bias}}(t) - \min(\mathbf{F}^{\text{bias}}(t))}{\max(\mathbf{F}^{\text{bias}}(t)) - \min(\mathbf{F}^{\text{bias}}(t))} \times (\max_F^{\text{new}}(i) - \min_F^{\text{new}})$$

The process is repeated until all negative values are removed and the alignment between historical and future data is within a desired tolerance ($\Delta M(t = 2010, i) \leq 0.01$, which is equivalent to an acceptable error of 1%).

4: Amplitude Correction

Some sectors, such as livestock, manufacturing and mining, do not have any seasonality in the datasets we use, therefore no amplitude correction is needed. For sectors that require such a correction (domestic, electric, and irrigation), we adjust $\mathbf{F}^{\text{bias, rescaled}}(t)$ to correct the amplitude for each future year $t \geq 2010$.

For this, we first calculate the original amplitude of the bias-adjusted and rescaled future data for year t :

$$A_F^{bias, rescaled}(t) = \max(\mathbf{F}^{bias, rescaled}(t)) - \min(\mathbf{F}^{bias, rescaled}(t))$$

Then, for the overlapping year $t = 2010$, we rescale the future data using min-max normalization to match the historical amplitude:

$$\mathbf{F}^{bias, rescaled, amplitude}(t = 2010) = \left(M_H^{2010} - \frac{A_H^{avg}}{2}\right) + \frac{\mathbf{F}^{bias, rescaled}(t = 2010) - \min(\mathbf{F}^{bias, rescaled}(t = 2010))}{A_F^{bias, rescaled, 2010}} \times A_H^{avg}$$

This procedure ensures that for the overlapping year 2010, both the historical and future datasets have the same middle point and amplitude. For future years $t > 2010$, the rescaling is performed based on the amplitude of the previous year amplitude in the calculation. It should be noted that, in comparison to the negative values rescaling correction, the amplitude correction is done for each year separately instead of the entire time-series at once. For this, we define the new minimum and maximum values as:

$$\min_F^{new, amplitude}(t) = M_F^{bias, rescaled}(t) - \frac{A_F^{bias, rescaled}(t)}{A_F^{bias, rescaled}(t-1)} \times \frac{A_F^{bias, rescaled, amplitude}(t-1)}{2}$$

$$\max_F^{new, amplitude}(t) = M_F^{bias, rescaled}(t) + \frac{A_F^{bias, rescaled}(t)}{A_F^{bias, rescaled}(t-1)} \times \frac{A_F^{bias, rescaled, amplitude}(t-1)}{2}$$

As we can see, in this definition of $\min_F^{new, amplitude}(t)$ and $\max_F^{new, amplitude}(t)$ we have a multiplication factor $\frac{A_F^{bias, rescaled}(t)}{A_F^{bias, rescaled}(t-1)}$ which is based on the relative difference between current and previous year amplitudes for the bias adjusted and negative values rescaled future time-series. It is through this that we allow the amplitude corrected dataset to experience the same year-to-year relative change in the amplitude compared to the original future data, while for the year 2010 the magnitude of the amplitude is equal to A_H^{avg} .

With the newly defined minimum and maximum values, we simply rescale each year accordingly:

$$\mathbf{F}^{bias, rescaled, amplitude}(t) = \min_F^{new, amplitude}(t) + \frac{\mathbf{F}^{bias, rescaled}(t) - \min(\mathbf{F}^{bias, rescaled}(t))}{A_F^{bias, rescaled}(t)} \times A_F^{bias, rescaled, amplitude}(t)$$

where $A_F^{bias, rescaled, amplitude}(t)$ is calculated as usual:

$$A_F^{bias, rescaled, amplitude}(t) = \max_F^{new, amplitude}(t) - \min_F^{new, amplitude}(t)$$

5. Final Output

The final corrected future data $\mathbf{F}^{final}(t)$ are given by:

$$\mathbf{F}^{final}(t) = \mathbf{F}^{bias, rescaled}(t)$$

or

$$\mathbf{F}^{final}(t) = \mathbf{F}^{bias, rescaled, amplitude}(t)$$

3. Results

3.1 Domestic Sector

3.1.1 National level time-series continuity

As described in Section 2.5.1, the primary issues identified in the original datasets include discontinuities in mean annual values (e.g. Belgium, Moldova, in Fig. 3) and abrupt changes in seasonality amplitude at the transition year (e.g., notably for Texas in Fig. 3). However, it is important to note that there are also instances when the future time-series transitions smoothly in terms of both annual mean values and seasonality (e.g., China, India, in Fig. 3). While only showing a subset, these time-series have been generated for each country and US state.

After applying the proposed harmonization algorithm (Table 3), we confirm that the national/state time-series are fully harmonized between the historical and future periods (Fig. 3). At the global level (Fig. 4), we observe that the domestic withdrawal time-series from Khan et al. (2023) [44] closely matches the reconstruction by Huang et al. (2018) [37], with only a slight overestimation. This overestimation is completely corrected in the harmonized dataset (Fig. 4).

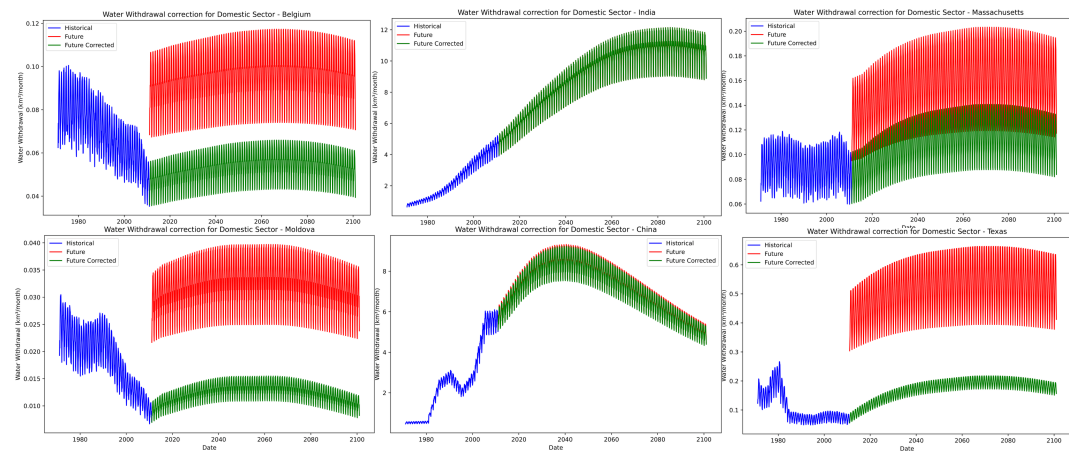


Figure 3. Original and corrected national/state monthly domestic withdrawal time-series. For this example, future data is based on the SSP2-RCP2.6-GFDL scenario.

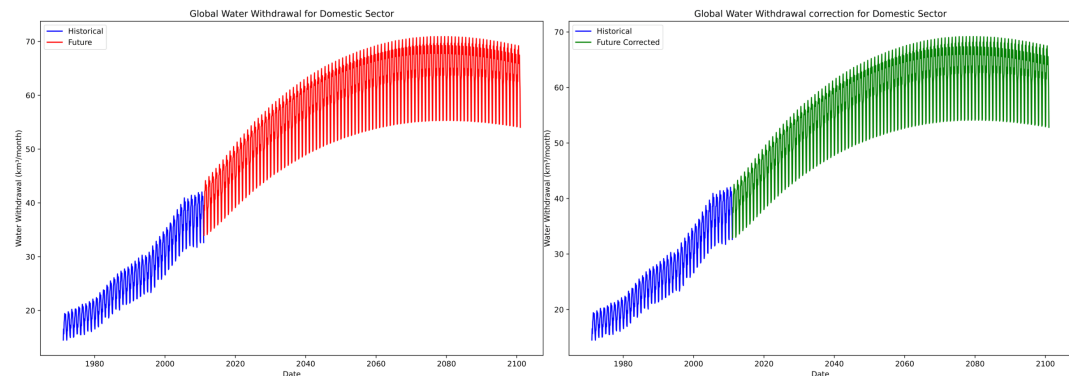


Figure 4. Original and corrected global monthly domestic withdrawal time-series. For this example, future data is based on the SSP2-RCP2.6-GFDL scenario.

3.1.2 Spatial consistency

To confirm the harmonization of past and future datasets, the final step is to verify spatial consistency at the transition between these periods. Continuity should be expected not only at the national/state level but also at the gridcell level, as described in Section 2.4.

For domestic water withdrawals, we observe that the original future dataset shows significant relative differences across most regions (Fig. 5). These differences are largely homogeneous and confined within national borders, indicating an issue with continuity at the national/state level. In fact, when we examine the same maps for the harmonized national/state data (Fig. 5), most of these discrepancies disappear. This high level of spatial consistency can be attributed to the fact that both Huang et al. (2018) [37] and Khan et al. (2023) [44] use the same downscaling map.

However, there are still some grid cells where the original high relative differences remain for the transition years 2010–2011 (Fig. 5). These correspond to insular countries that were not included in the country mask used for the harmonization process. Although it is possible to extend the algorithm to cover these cases, doing so would significantly complicate the workflow without an updated mask file. Therefore, for users in affected island countries, we recommend applying the same harmonization algorithms described here after updating the mask file to include their region.

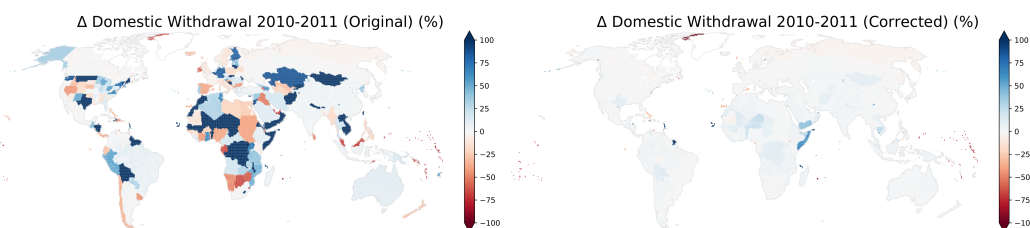


Figure 5. Year 2010–2011 relative change in domestic withdrawal calculated at gridcell level from the historical, and original (left) or harmonized (right) future data. For this example, future data is based on the SSP2-RCP2.6-GFDL scenario.

3.2 Livestock Sector

3.2.1 National level time-series continuity

Unlike the domestic sector, the national livestock time-series exhibit discontinuities only in mean annual values at the transition between historical and future datasets. Since both the Huang et al. (2018) [37] reconstruction and the future scenarios from Khan et al. (2023) [44] downscale annual livestock water withdrawals using a uniform distribution (the same value is applied every month), there are no issues related to mismatches in seasonality amplitude.

Given this, we only applied a bias adjustment correction while ensuring no negative values (see Table 3). As a result, full continuity is achieved for each country and U.S. state where the correction was implemented (Fig. 6). Unlike the domestic sector, where the overall global impact was relatively small, harmonized livestock water withdrawals show a significant increase in future scenarios (Fig. 7).

3.2.2 Spatial consistency

Similar to the domestic sector, when examining the spatial distribution of relative changes, we observe significant differences during the transition year in the original dataset (Fig. 8). However, after applying the bias adjustment at the national and U.S. state levels, we still notice some jumps and drops at the grid cell level, particularly evident in the U.S. states (see, e.g., Fig. 8), which were not observed in the domestic sector.

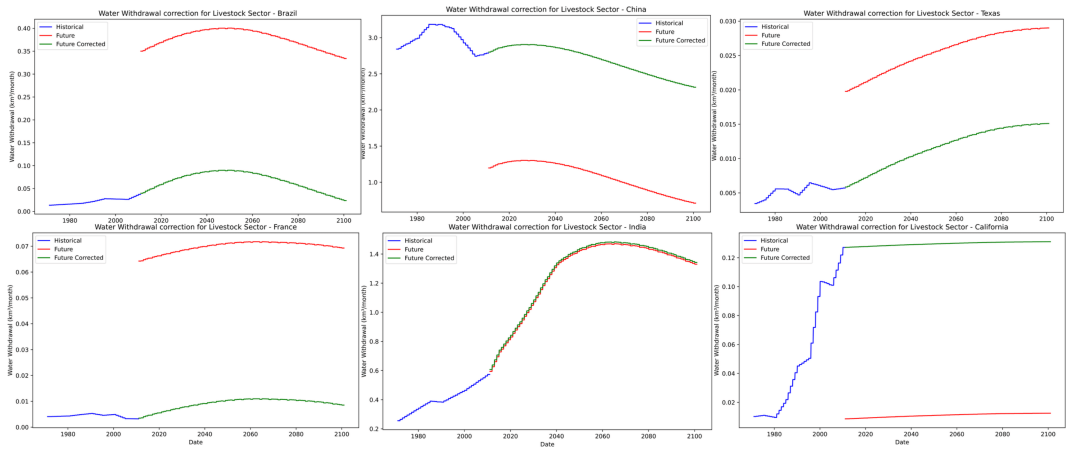


Figure 6. Original and corrected national/state monthly livestock withdrawal time-series. For this example, future data is based on the SSP2-RCP2.6-GFDL scenario.

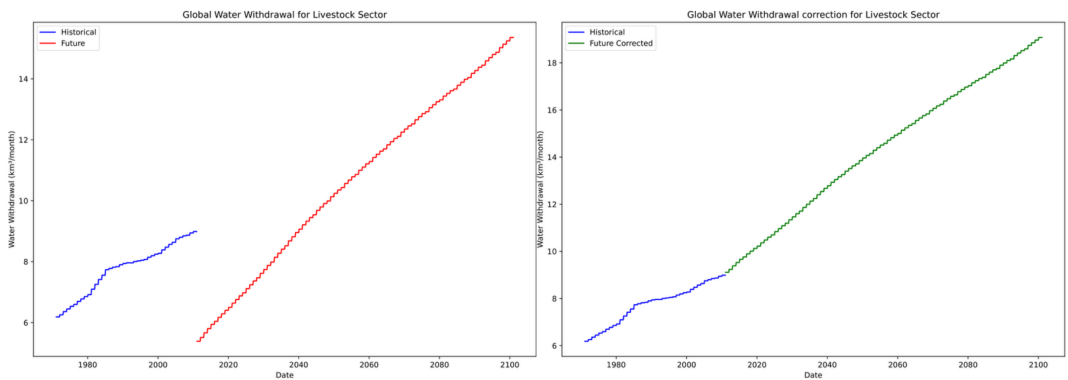


Figure 7. Original and corrected global monthly livestock withdrawal time-series. For this example, future data is based on the SSP2-RCP2.6-GFDL scenario.

Although one might argue that such gridcell differences are acceptable, as they could reflect temporal changes in livestock densities (if accounted for), in this case, both the historical and future datasets use the same 2005 FAO livestock density map for spatial downscaling (Section 2.2). The differences are due solely to variations in the methodology used to translate individual livestock density maps into downscaling weights for the entire sector.

Given that the same downscaling proxy is used, we conclude that these gridcell differences do not provide any meaningful insights and should be harmonized. To achieve this, we propose a simple algorithm. First, for the future dataset, we calculate each gridcell's weight based on the total national or U.S. state-level annual livestock withdrawal for the year 2010. Next, we downscale the historical national and U.S. state monthly time-series to the grid level using the weights generated in the first step. The result is a spatially harmonized dataset that preserves the original national or U.S. state-level totals while adjusting their gridcell distribution. The final results show a level of spatial consistency similar to that achieved for the domestic sector (Fig. 9).

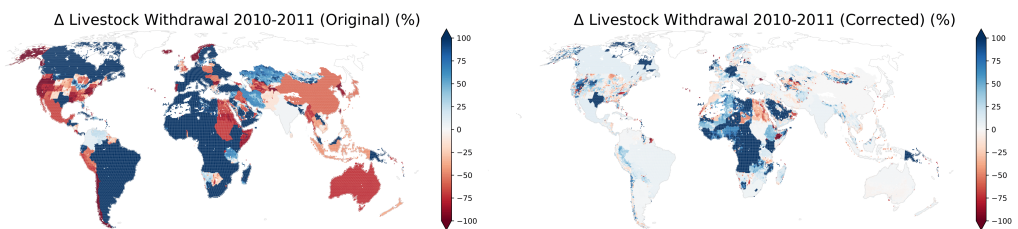


Figure 8. Year 2010–2011 relative change in livestock withdrawal calculated at gridcell level from the original historical, and original (left) or harmonized (right) future data. For this example, future data is based on the SSP2-RCP2.6-GFDL scenario. (to change figure with similar format to the other spatial figures)

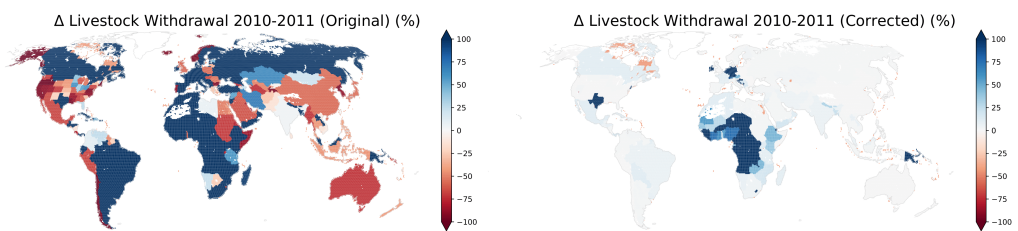


Figure 9. Year 2010–2011 relative change in livestock withdrawal calculated at gridcell level from the downscaling corrected historical, and original (left) or harmonized (right) future data. For this example, future data is based on the SSP2-RCP2.6-GFDL scenario.

3.3 Electric Sector

3.3.1 National level time-series continuity

For the electric sector, we confirm the successful harmonization of the historical and future time-series at the country level (Fig. 10). The seasonality has been effectively adjusted, with corresponding increases (e.g., Egypt, U.S. Alabama) or decreases (e.g., Denmark, U.S. Florida) in amplitude in the future time-series. Furthermore, we have successfully preserved the original relative importance of the values for each month (for example, the peak-to-peak correspondence for Azerbaijan).

However, in some cases, it is not always possible to fully maintain the original trend. For example, in the case of U.S. Florida, while the overall trend is preserved, with a decreasing pattern until 2060 followed by an increase, the amplitude of the trend variation is much smaller. This is due to the negative value correction algorithm. When the future time-series exhibits a much larger variation (i.e., the difference between the maximum and minimum values for the entire time-series) compared

to the historical period, the algorithm gradually compresses the trend to ensure continuity in mean values and amplitude, while also preventing negative values. Although such changes are inevitable to ensure consistency, they may indicate underlying issues with one of the datasets. For instance, it is possible that historical values for U.S. Florida are too low, or that certain assumptions in the design of future scenarios for the region may need to be revised.

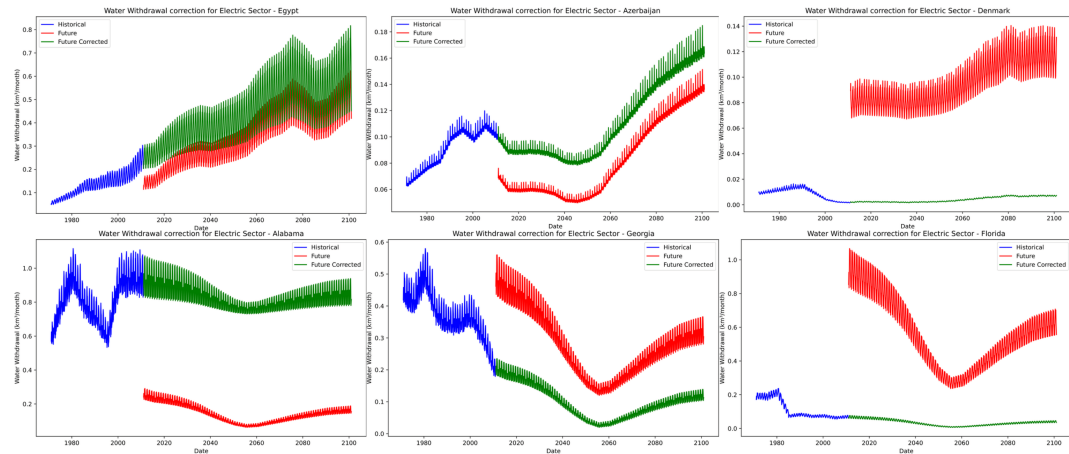


Figure 10. Original and corrected national/state monthly electric withdrawal time-series. For this example, future data is based on the SSP2-RCP2.6-GFDL scenario.

On the global scale, the harmonization procedure demonstrates a clear added value, resulting in a perfect match at the transition year in the corrected version (Fig. 11).

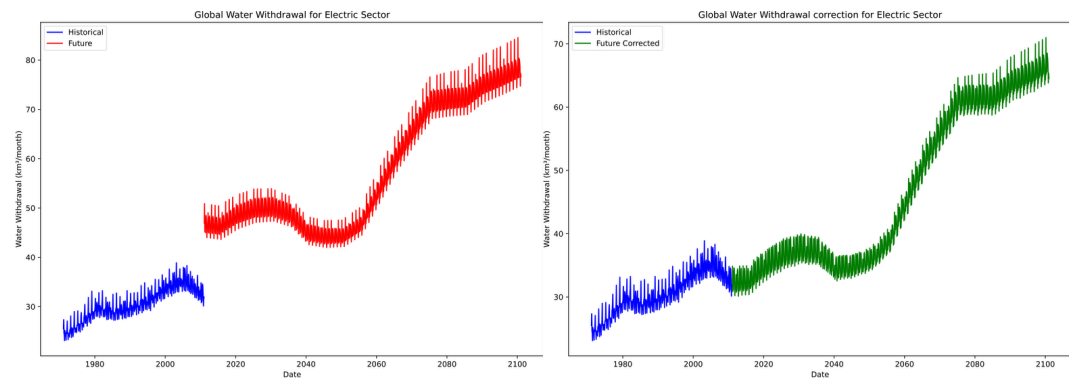


Figure 11. Original and corrected global monthly electric withdrawal time-series. For this example, future data is based on the SSP2-RCP2.6-GFDL scenario.

3.3.2 Spatial consistency

We also confirm the spatial consistency of the harmonized dataset, with reasonable relative changes at the transition year (2010–2011) for most countries (Fig. 12). However, there are a few notable exceptions (e.g., Bolivia, Mali, Somalia, and Tanzania). In all these cases, the historical time-series show values close to zero, followed by a rapid increase in the future projections, which explains the large positive relative change.

3.4 Manufacturing and mining sector

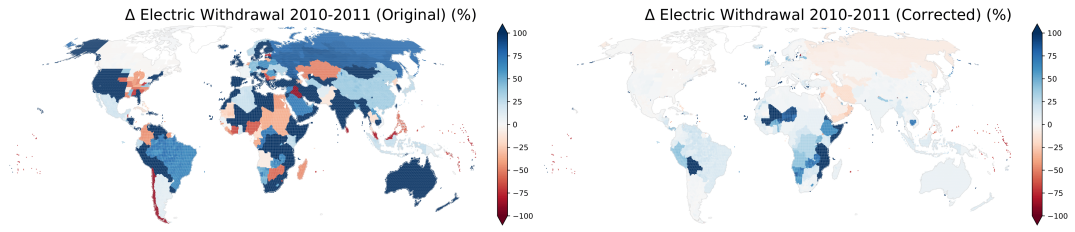


Figure 12. Year 2010–2011 relative change in electric withdrawal calculated at gridcell level from the original historical, and original (left) or harmonized (right) future data. For this example, future data is based on the SSP2-RCP2.6-GFDL scenario.

3.4.1 National level time-series continuity

Successful harmonization has been achieved for the manufacturing and mining sector time-series at the country level (Fig. 13, 15). At the global level, the harmonized time-series are well aligned, significantly reducing the original gap at the transition period (Fig. 14, 16).

409
410
411
412

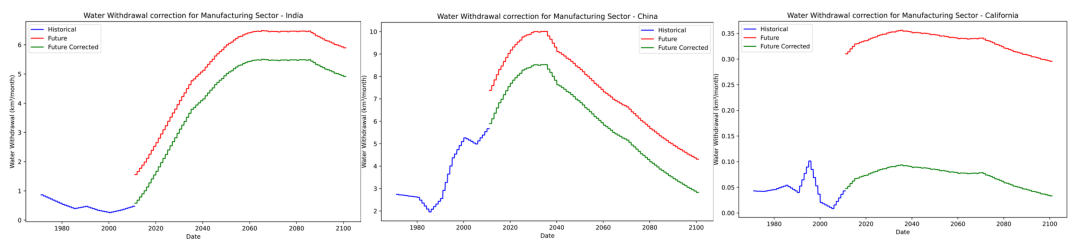


Figure 13. Original and corrected national/state monthly manufacturing withdrawal time-series. For this example, future data is based on the SSP2-RCP2.6-GFDL scenario.

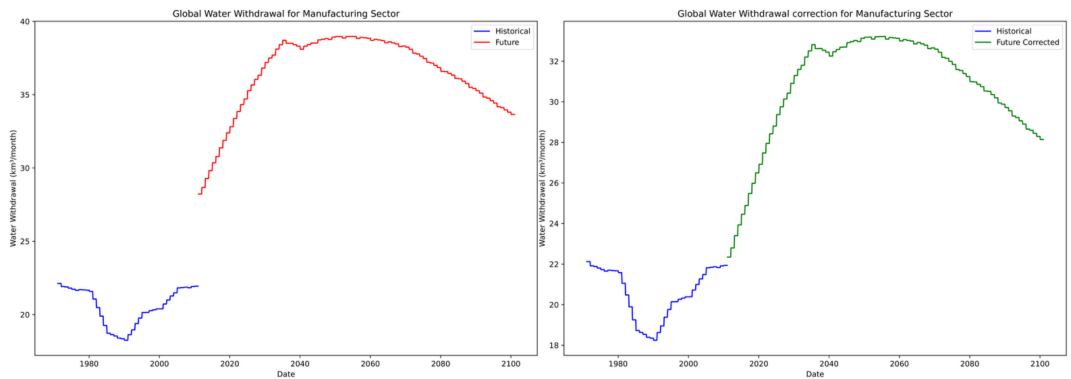


Figure 14. Original and corrected global monthly manufacturing withdrawal time-series. For this example, future data is based on the SSP2-RCP2.6-GFDL scenario.

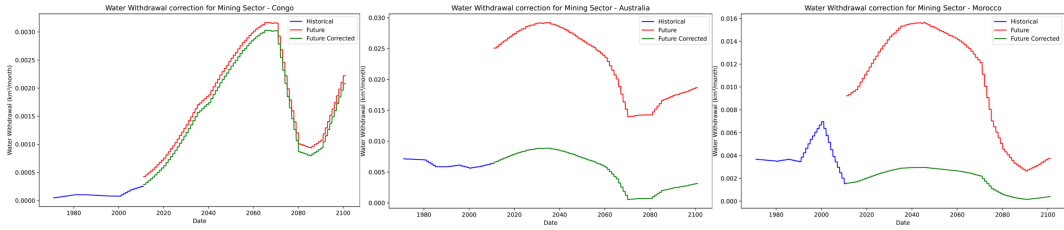


Figure 15. Original and corrected national/state monthly mining withdrawal time-series. For this example, future data is based on the SSP2-RCP2.6-GFDL scenario.

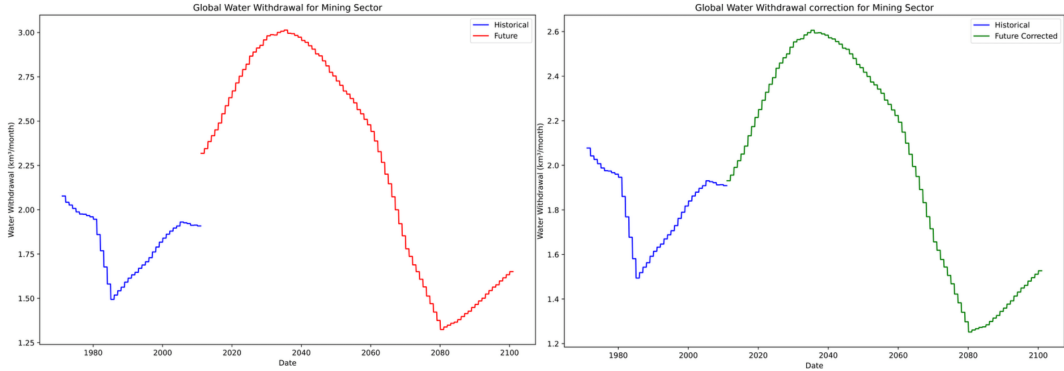


Figure 16. Original and corrected global monthly mining withdrawal time-series. For this example, future data is based on the SSP2-RCP2.6-GFDL scenario.

3.4.2 Spatial consistency

Spatially, we find the resulting harmonized data to be very consistent, without the need for additional interventions (Fig. 17-18).

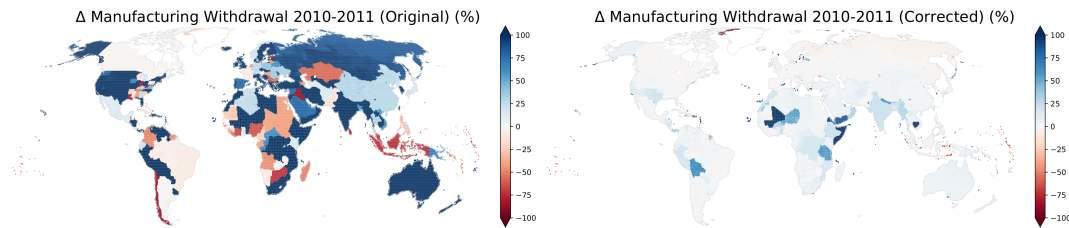


Figure 17. Year 2010–2011 relative change in manufacturing withdrawal calculated at gridcell level from the original historical, and original (left) or harmonized (right) future data. For this example, future data is based on the SSP2-RCP2.6-GFDL scenario.

3.5 Irrigation Sector

3.5.1 National level time-series continuity

The harmonization procedure performed well for the irrigation sector (Fig. 19). In the examples provided, as well as for other countries, we observe that the seasonality amplitude in the future dataset at the transition year is well-aligned with the latest historical period and generally improved compared to the original data. However, one behaviour that occasionally emerges, and whose physical plausibility might be questioned, is when the corrected time-series shows no zero values (e.g., Lebanon), despite the original future data containing zero values. For now, we accept this behaviour,

413
414
415

416
417
418
419
420
421
422
423

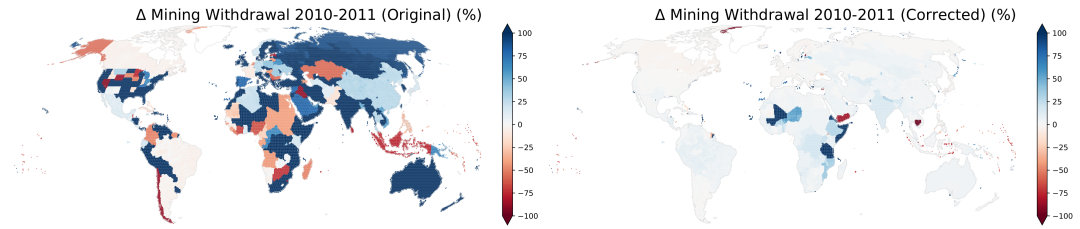


Figure 18. Year 2010–2011 relative change in mining withdrawal calculated at gridcell level from the original historical, and original (left) or harmonized (right) future data. For this example, future data is based on the SSP2-RCP2.6-GFDL scenario.

as it also appears in some cases within the original future data (e.g., Pakistan, Burundi). However, in the future, we could consider revising the algorithm for the irrigation sector. One potential improvement would be to enforce zero values during the rescaling process for amplitude correction if zero values were present in both the historical and original future time-series.

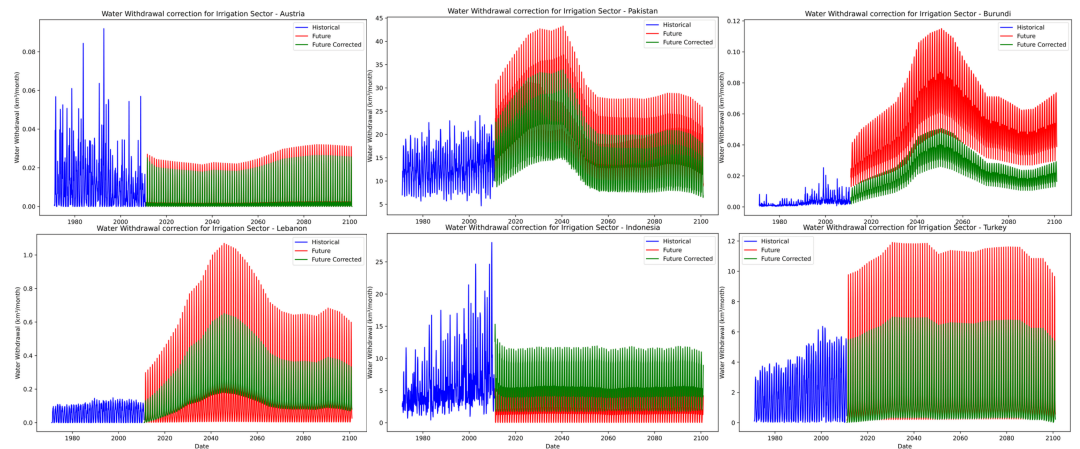


Figure 19. Original and corrected national/state monthly irrigation withdrawal time-series. For this example, future data is based on the SSP2-RCP2.6-GFDL scenario.

At the global level, the harmonization process effectively aligned the time-series, making the transition period appear more realistic (Fig. 20).

3.5.2 Spatial consistency

In terms of spatial consistency at the transition year, we observe a significant improvement in the harmonized dataset compared to the original future dataset (Fig. 21). However, the alignment is not perfect. This is largely due to the fact that annual irrigation withdrawals at the grid-cell level can vary significantly from year to year, making gradual changes less applicable in this context. Additionally, differences in the downscaling methodologies between the historical and future datasets (Sections 2.1 and 2.2) likely contribute, as a grid cell might be allocated for irrigation in one dataset but not in the other.

Using a relative change for only one year does not fully disentangle the contributions of these two mechanisms. A clearer understanding could be gained by comparing relative changes over aggregated time periods (e.g., 2005–2010 vs. 2011–2016) or by applying a rolling average approach. Nevertheless, unlike in the livestock sector, we do not apply any downscaling corrections here due to the uncertainty of the mechanisms described.

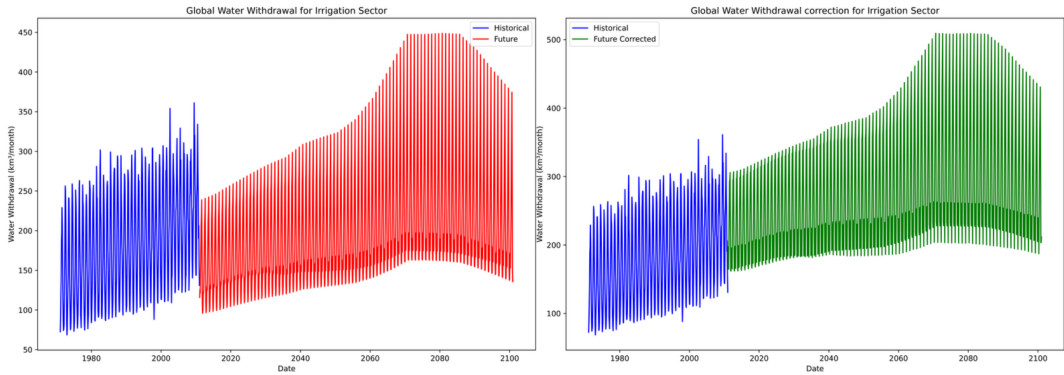


Figure 20. Original and corrected global monthly irrigation withdrawal time-series. For this example, future data is based on the SSP2-RCP2.6-GFDL scenario.

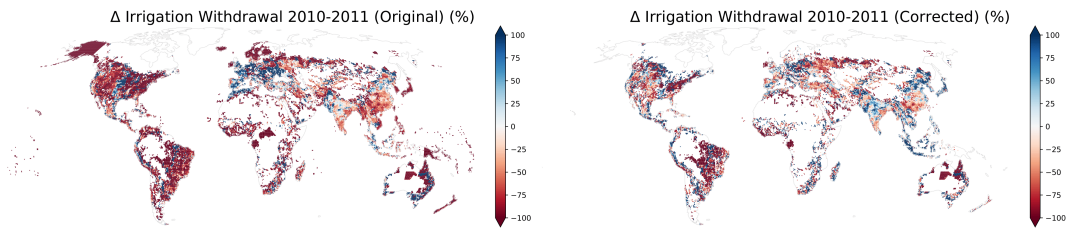


Figure 21. Year 2010–2011 relative change in irrigation withdrawal calculated at gridcell level from the original historical, and original (left) or harmonized (right) future data. For this example, future data is based on the SSP2-RCP2.6-GFDL scenario.

3.6 Ensemble View

By applying our methodology to all the selected scenarios (Table 1), we confirm the successful harmonization of the historical and future periods (Fig. 22). For all sectors except domestic, we observe significant differences between the pre- and post-harmonized datasets, underscoring the importance of harmonizing historical and future data before use. The most notable change occurs in the irrigation sector, where the original scenario data severely underestimates global annual withdrawals, with 2010 values comparable to those of the 1970s and 1980s. In general, both underestimations (domestic, irrigation, livestock) and overestimations (electric, manufacturing, mining) of sectoral withdrawals are possible. If left uncorrected, such inconsistencies may propagate into water-related research, potentially affecting the outputs of GHMs/ESMs that rely on sectoral water abstraction inputs.

443
444
445
446
447
448
449
450
451
452
453

Global Sectoral Time Series: Corrected vs Original (in km³/year)

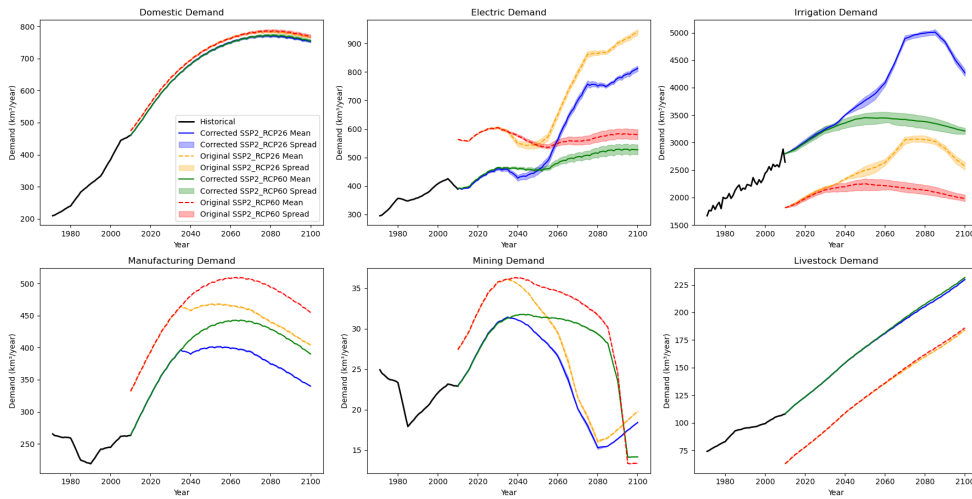


Figure 22. Comparison of global time-series of sectoral water use aggregated at annual level before and after harmonization for the selected ensemble of scenarios (Table 1).

4. Discussion

One of the critical challenges in using socio-economic datasets for water resource modelling is the presence of spatial and temporal inconsistencies, particularly at the transition between historical and future periods. These inconsistencies, which manifest as sudden jumps or drops in mean values and seasonality at the transition year, can severely affect the reliability of research and modelling outcomes. Temporal inconsistencies occur when historical time-series data fail to align smoothly with future projections, creating artificial shifts in trends. Spatial inconsistencies arise when the downscaling of national or regional data is handled differently for historical and future datasets, leading to misalignments at the grid-cell level. Both issues can introduce biases into models that rely on these datasets, such as Global Hydrological Models (GHMs) and Earth System Models (ESMs), resulting in misleading conclusions about future water availability and human-water interactions.

To address these challenges, we implemented a harmonization process to ensure spatial and temporal consistency between historical and future sectoral water use data. By carefully examining and correcting for biases in both mean values and seasonality at the transition year, we were able to align time-series data at national and sub-national levels across multiple sectors, including domestic, irrigation, electric, manufacturing, livestock, and mining. The process involved identifying and rectifying significant discrepancies, such as abrupt changes in withdrawal values and shifts in seasonality amplitude, which would otherwise undermine the reliability of future projections.

The harmonization approach we applied is particularly beneficial for improving the accuracy of models that depend on socio-economic inputs, like water use data, to simulate future scenarios. For instance, without harmonization, models might propagate incorrect assumptions about future water demands, which could skew projections of water scarcity or stress. By ensuring that these datasets are temporally and spatially aligned, our methodology allows for more reliable interpretations of future water trends, contributing to more informed policy decisions and resource management strategies.

Looking forward, preventing such inconsistencies from arising requires a more concerted effort

454
455
456
457
458
459
460
461
462
463
464
465
466
467
468
469
470
471
472
473
474
475
476
477
478

across several fronts. First, there is a need for greater collaboration between the centres and organizations responsible for designing socio-economic data products. Often, historical data and future projections are developed independently, with little coordination regarding methodologies or assumptions. Ensuring that these efforts are better aligned, particularly when transitioning from observed data to modelled projections, will help reduce discrepancies.

Second, robust quality control protocols should be established to check both spatial and temporal consistency during dataset production. Although individual datasets may be validated for accuracy in isolation, they often reveal inconsistencies when combined across time periods or regions. Implementing standard benchmarks for evaluating consistency at multiple scales, from national to grid-cell level, would help catch and address these issues early in the development process.

Finally, there is a growing need for harmonization efforts to be prioritized when datasets developed by different centers are intended for downstream use in modeling frameworks. Independent dataset creation, while often necessary due to specific regional or sectoral focuses, can result in fragmented outputs that are difficult to integrate. Harmonizing these datasets to ensure smooth transitions between historical and future periods will make them more reliable for downstream users, such as GHMs and ESMs, which depend on seamless data for accurate projections.

Appendix 1. Inconsistent population input data in ISIMIP2 at the transition between historical and future periods

Appendix 1.1 Country population time-series

In general, for many countries, the national population time-series are continuous and free of anomalies (e.g., Fig. 23). In such cases, no correction to the national time-series is required.

On the other hand, some countries' national time-series exhibit significant jumps or drops between 2005 and 2010. Rather than bias-adjusting the future or historical time-series, the dataset appears to have been merged using linear interpolation for this period. While this approach yielded acceptable results in many cases, there are approximately 40–50 exceptions in the specific dataset examined (ISIMIP2 population for historical and SSP2 scenario, see e.g., Fig. 24).

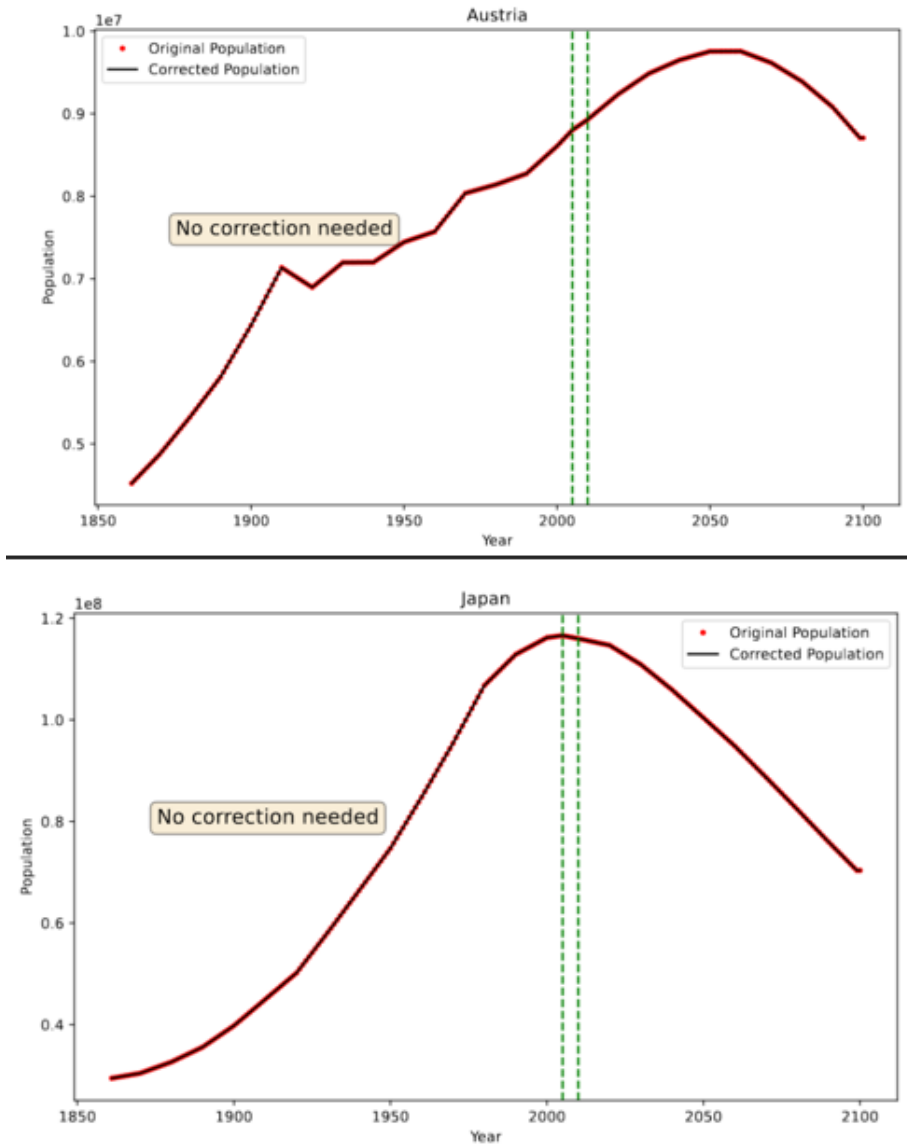


Figure 23. Examples of correct population time-series from ISIMIP2 protocol aggregated at country level.

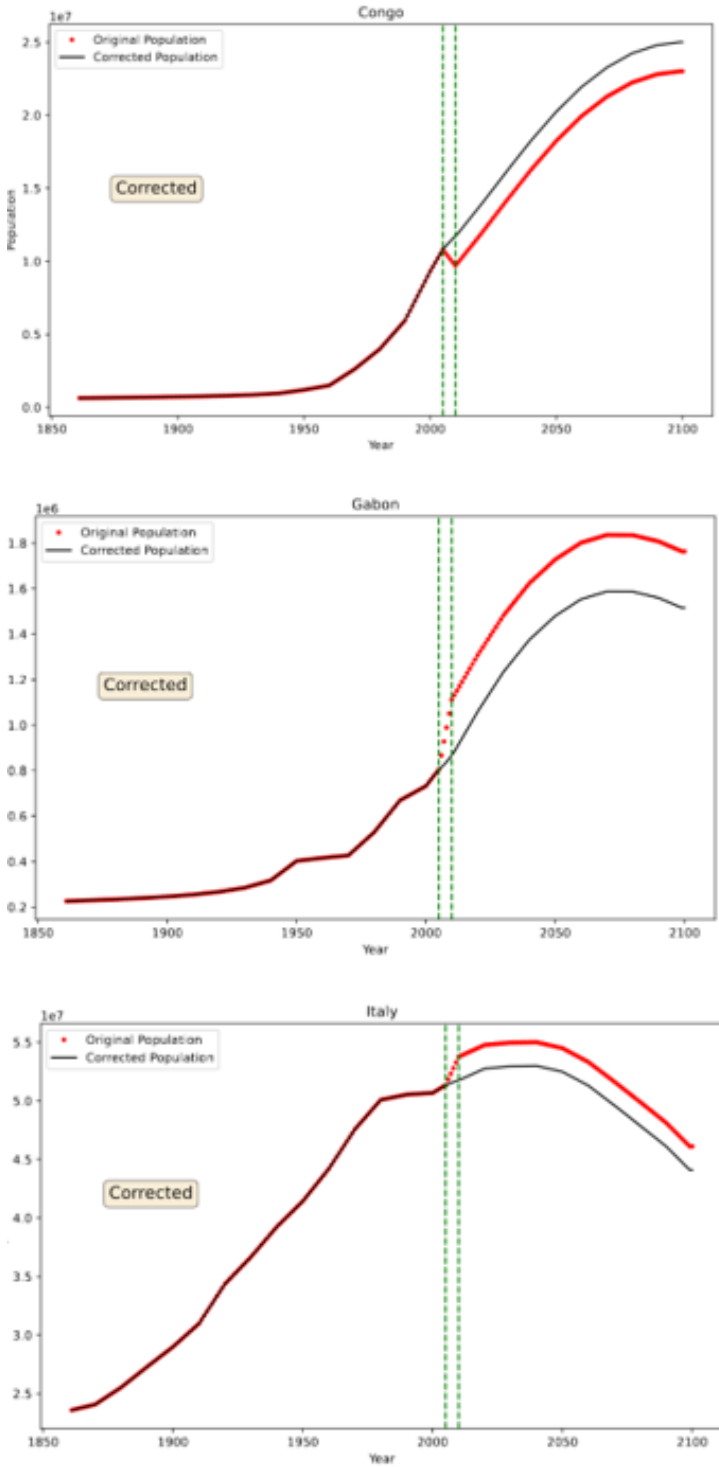


Figure 24. Examples of incorrect population time-series from ISIMIP2 protocol aggregated at country level that were corrected by our approach.

Appendix 1.2 Spatial inconsistency within a country or grid-level time-series inconsistency

In addition to the occasional issues with national population time-series, the dataset exhibits another problem: spatial inconsistency after 2005. Specifically, at the transition between historical and future datasets, the population within a country appears to be redistributed among its grid cells at the transition year 2005–2006 (Fig. 25).

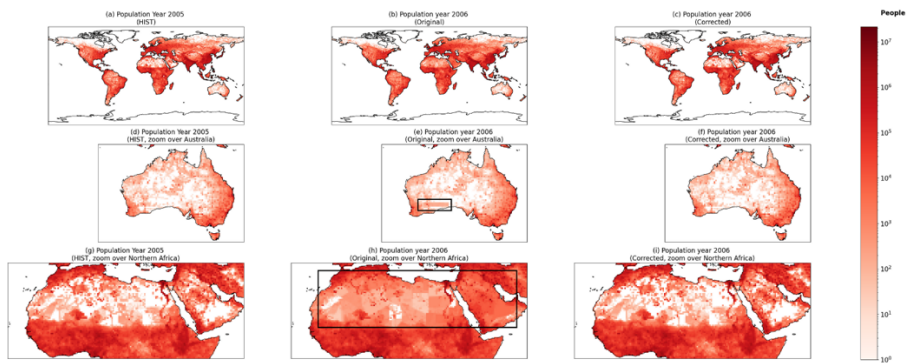


Figure 25. Examples of spatial inconsistencies in the population data from the ISIMIP2 protocol.

Appendix 1.3 Harmonizing population data in ISIMIP2

To address this issue, we apply a straightforward harmonization procedure consisting of the following steps:

1. Correct National Time-Series Biases: Instead of using linear interpolation between the 2005 historical and 2100 future scenario years, we adjust the 2100 value up or down to align with the expected trend. This adjustment is based on the rate of change observed in the last few historical years and the first few future years, ensuring a smoother transition.
2. Compute Gridcell Weights: For each grid cell within a country, we calculate its weight, representing the fraction of the country's population contained within that specific grid cell. For example, if a grid cell has a weight of 0.1, it means that 10% of the country's population resides in that grid cell.
3. Downscale Future National Population: Using the gridcell weights from the last historical year (2005), we distribute the future national population (2006–2100) proportionally across the grid cells, maintaining the spatial distribution from the historical dataset.

The limitation of this approach is that the weights within a country remain constant from 2005 onwards. This implies that the relative importance of each grid cell in the population distribution does not change over time. This assumption is unrealistic, as factors such as war, flooding, fires, and socio-economic opportunities cause certain cities or regions to grow or shrink at varying rates. In reality, grid cell weights should dynamically evolve to reflect these localized changes in population distribution over time.

Unfortunately, addressing this issue in a meaningful and accurate way would require the implementation of more complex correction algorithms. Ideally, such adjustments should be made by the dataset developers themselves, as they have the most comprehensive understanding of the assump-

tions and methodologies underpinning the data creation process.

The advantage of our approach is that it produces a spatially consistent population dataset with more continuous time-series at the grid cell level. These time-series align with the national population trends prescribed by the SSP scenarios, enabling grid-cell-based analysis. Additionally, this harmonized dataset can be used as input for Global Hydrological Models (GHMs) without the risk of introducing errors into the outputs.

The success of the spatial harmonization is confirmed in Fig. 26-27.

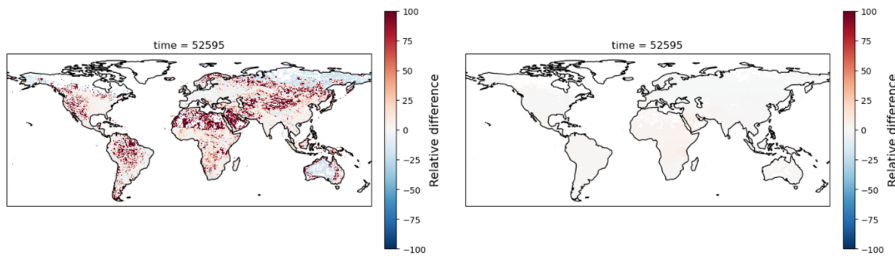


Figure 26. The relative difference in population count between the transition years 2005 and 2006 is shown as a percentage of the 2005 values. On the left, the original data reveal notable inconsistencies, while on the right, the differences after correction demonstrate that full spatial consistency has been achieved through the harmonization process.

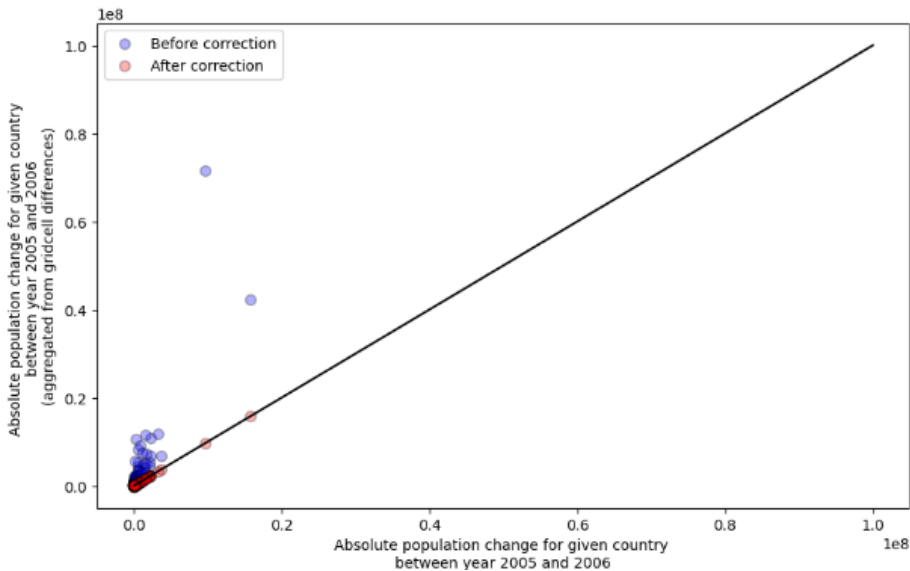


Figure 27. The correlation plot compares the absolute change in population count for each country between the transition years 2005 and 2006, calculated using two methods. On the x-axis, the population is aggregated at the country level for each year, and the difference is computed. On the y-axis, differences are calculated at the grid cell level, and the sum of all contributions is obtained. A perfect match between the two methods would indicate spatial consistency in the data. Deviations from this relationship suggest spatial inconsistencies, where grid cell-level contributions do not align with country-level changes, likely due to reorganization of individual grid cell weights.

While this analysis focused on ISIMIP2 population data, we observed similar issues in ISIMIP3 population data.

540

541

542

543

544

545

546

547

548

549

550

Appendix 1.4 Inconsistent water use data in ISIMIP2 and ISIMIP3

551

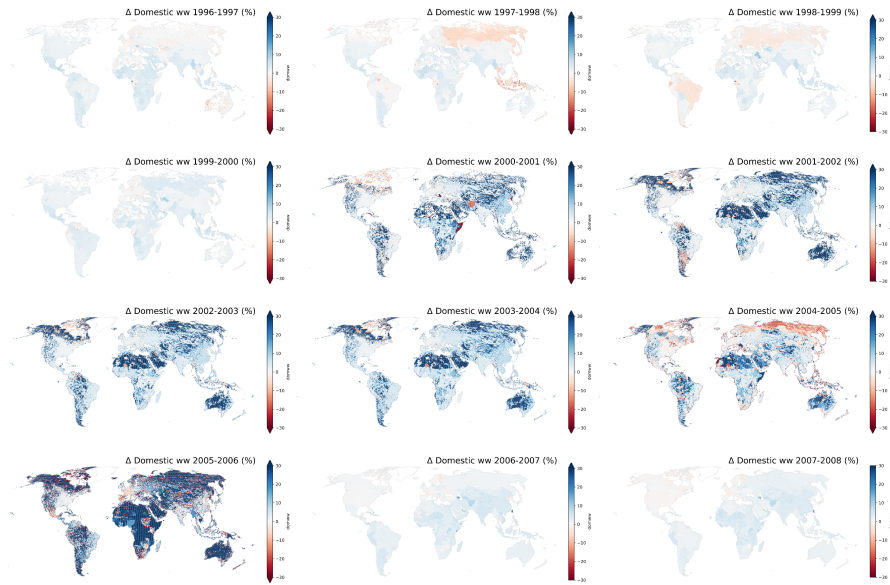


Figure 28. The relative difference in water withdrawal for the domestic sector, calculated for the ensemble of ISIMIP2 models under SSP2-RCP2.6, represents the year-to-year percentage change compared to the previous year. This metric helps identify abrupt transitions or inconsistencies in the time-series, particularly at the historical-future interface.

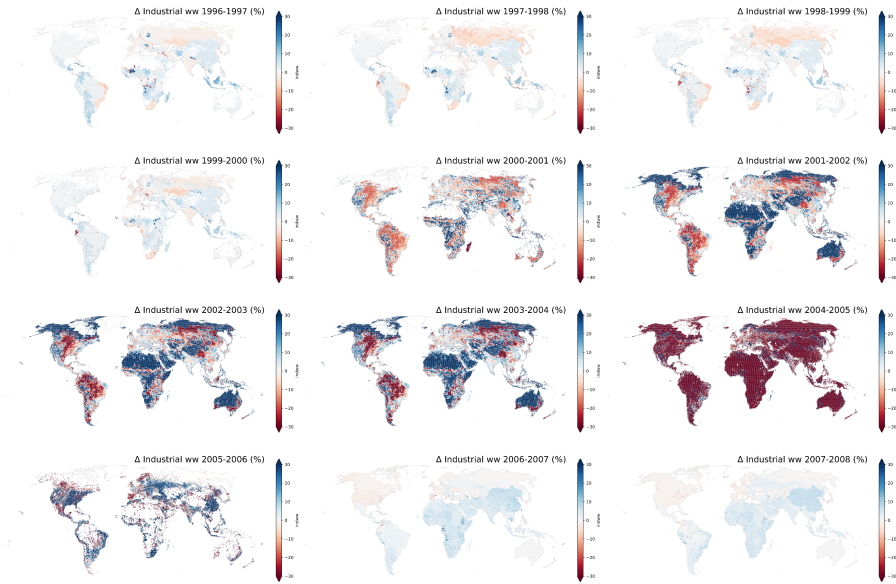


Figure 29. The relative difference in water withdrawal for the industrial sector, calculated for the ensemble of ISIMIP2 models under SSP-RCP2.6, represents the year-to-year percentage change compared to the previous year. This metric helps identify abrupt transitions or inconsistencies in the time-series, particularly at the historical-future interface.

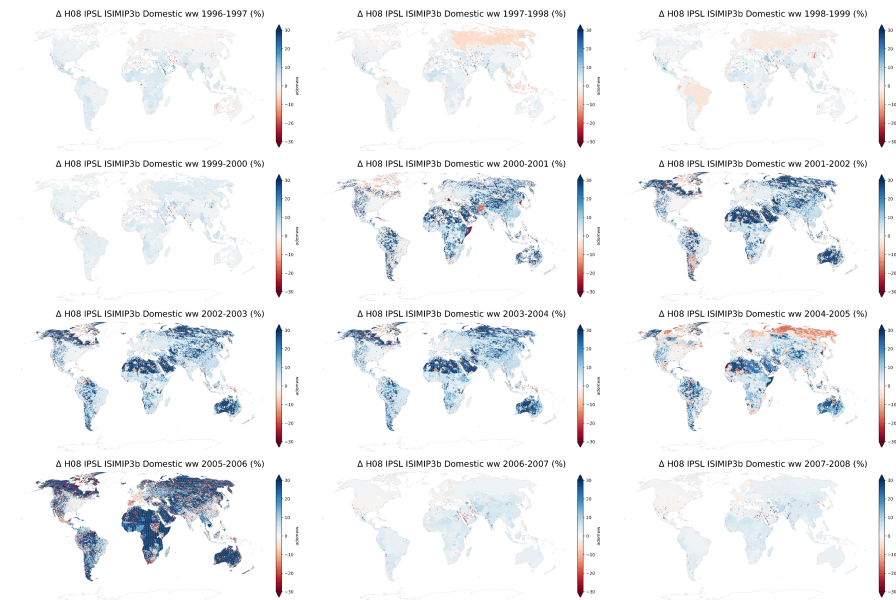


Figure 30. The relative difference in water withdrawal for the domestic sector, calculated for the ISIMIP3 H08-IPSL simulation under SSP2-RCP2.6, represents the year-to-year percentage change compared to the previous year. This metric helps identify abrupt transitions or inconsistencies in the time-series, particularly at the historical-future interface.

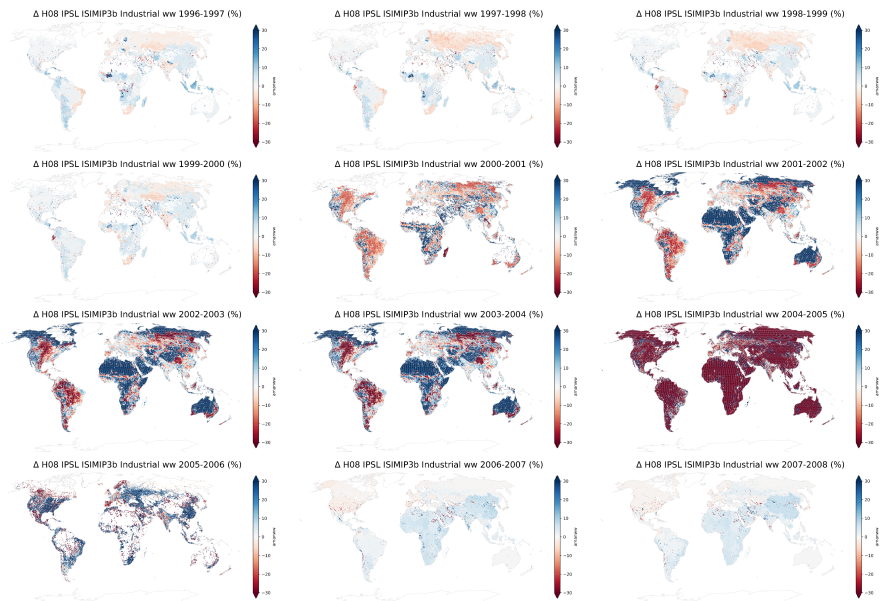


Figure 31. The relative difference in water withdrawal for the industrial sector, calculated for the ISIMIP3 H08-IPSL simulation under SSP2-RCP2.6, represents the year-to-year percentage change compared to the previous year. This metric helps identify abrupt transitions or inconsistencies in the time-series, particularly at the historical-future interface.

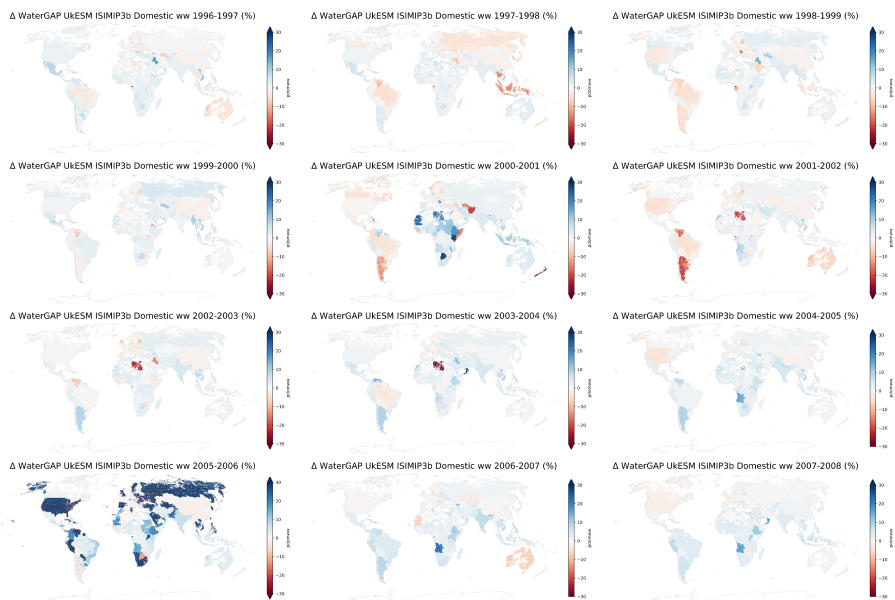


Figure 32. The relative difference in water withdrawal for the domestic sector, calculated for the ISIMIP3 WaterGAP-UkESM simulation under SSP2-RCP2.6, represents the year-to-year percentage change compared to the previous year. This metric helps identify abrupt transitions or inconsistencies in the time-series, particularly at the historical-future interface.

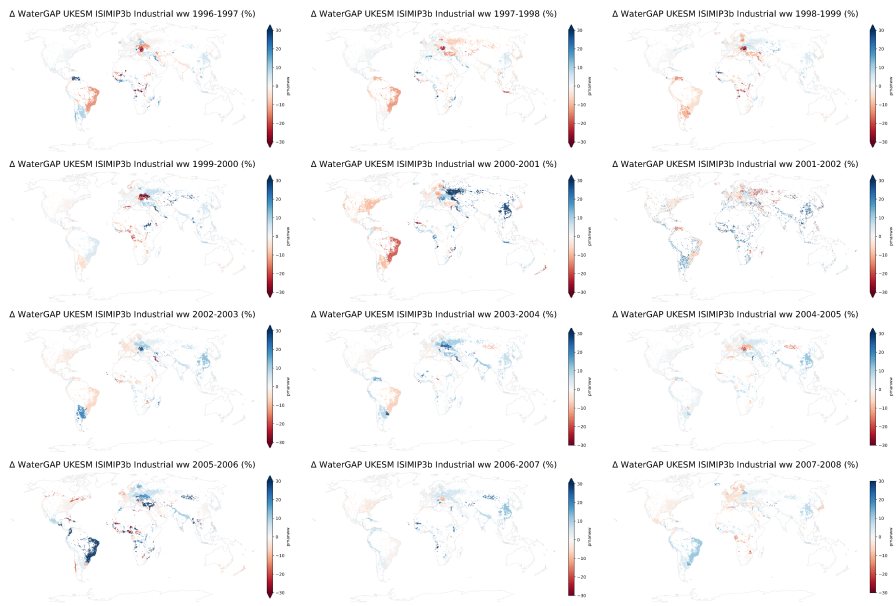


Figure 33. The relative difference in water withdrawal for the industrial sector, calculated for the ISIMIP3 WaterGAP-UkESM simulation under SSP2-RCP2.6, represents the year-to-year percentage change compared to the previous year. This metric helps identify abrupt transitions or inconsistencies in the time-series, particularly at the historical-future interface.

Acknowledgement

ChatGPT (GPT-4; OpenAI's large-scale language-generation model) was used to improve the writing style of this article. Sabin I. Taranu reviewed, edited, and revised the ChatGPT-generated texts to his own liking and ultimately takes responsibility for the content of this publication.

Author contributions

- Ioan Sabin Taranu: Conceptualization, Data Curation, Formal Analysis, Investigation, Methodology, Validation, Visualization, Writing (Original Draft)
- Inne Vanderkelen: Formal Analysis, Investigation, Visualization, Writing (Review and Editing)
- Yoshihide Wada: Supervision, Writing (Review and Editing)
- Ting Tang: Supervision, Writing (Review and Editing)
- Steven Eisenreich: Supervision, Writing (Review and Editing)
- Ann Van Griensven: Funding Acquisition, Supervision, Writing (Review and Editing)

Funding statement

The author has received funding from the European Union's Horizon 2021 research and innovation programme under the Marie Skłodowska-Curie grant agreement 956623, MSCA-ITN-ETN-European Training Network, inventWater Project (Inventive forecasting tools for adapting water quality management to a new climate).

Open data statement

If only the harmonization algorithm is of interest, then the best way to access it will be on GitHub (<https://github.com/TaranuDev/WaterUseDataHarmonization>). You will find there the code necessary to harmonize all the sectors for one historical/future water use combination.

To fully reproduce the study, you can download all the codes and data from the corresponding Zenodo repository (<https://doi.org/10.5281/zenodo.14850276>).

Another useful resource can be the population harmonization algorithm we introduce in the Appendix, as well as the investigation of ISIMIP2 and ISIMIP3 water use data. For this, you can check the corresponding GitHub repository (https://github.com/VUB-HYDR/isimip2b_population_correction).

Reproducibility statement

The materials to fully reproduce this study have been provided in the Open data statement.

References

- [1] M.M Mekonnen and A.Y. Hoekstra. “Four billion people facing severe water scarcity”. In: *Sci. Adv* (2016). doi: <https://doi.org/10.1126/sciadv.1500323>. 580
- [2] T. Oki and S. Kanae. “Global Hydrological Cycles and World Water Resources”. In: *Science* (2006). doi: <https://doi.org/10.1126/science.1128845>. 581
- [3] Y. Wada et al. “Modeling global water use for the 21st century: the Water Futures and Solutions (WFaS) initiative and its approaches”. In: *Geosci. Model Dev.* (2016). doi: <https://doi.org/10.5194/gmd-9-175-2016>. 582
- [4] M.T.H. Van Vliet, E.R. Jones, M. Flörke, W.H.P. Franssen, N. Hanasaki, Y. Wada, and J.R. Yearsley. “Global water scarcity including surface water quality and expansions of clean water technologies”. In: *Environ. Res. Lett.* (2021). doi: <https://doi.org/10.1088/1748-9326/abbfc3>. 583
- [5] C.J. Vörösmarty et al. “Global threats to human water security and river biodiversity”. In: *Nature* (2010). doi: <https://doi.org/10.1038/nature09440>. 584
- [6] M.T. Coe, M.H. Costa, and B.S. Soares-Filho. “The influence of historical and potential future deforestation on the stream flow of the Amazon River – Land surface processes and atmospheric feedbacks”. In: *Journal of Hydrology* (2009). doi: <https://doi.org/10.1016/j.jhydrol.2009.02.043>. 585
- [7] Y. Wada, L.P.H. Van Beek, and M.F.P. Bierkens. “Nonsustainable groundwater sustaining irrigation: A global assessment”. In: *Water Resources Research* (2012). doi: <https://doi.org/10.1029/2011WR010562>. 586
- [8] de Graaf IEM, Gleeson T, and Rens van Beek LPH. “Environmental flow limits to global groundwater pumping”. In: *Nature* (2019). doi: <https://doi.org/10.1038/s41586-019-1594-4>. 587
- [9] P.C.D. Milly, J. Betancourt, M. Falkenmark, R.M. Hirsch, Z.W. Kundzewicz, D.P. Lettenmaier, and R.J. Stouffer. “Stationarity Is Dead: Whither Water Management”. In: *Science* (2008). doi: <https://doi.org/10.1126/science.1151915>. 588
- [10] K. Trenberth. “Changes in precipitation with climate change”. In: *Clim. Res.* (2011). doi: <https://doi.org/10.3354/cr00953>. 589
- [11] P. Döll and H.M. Schmied. “How is the impact of climate change on river flow regimes related to the impact on mean annual runoff? A global-scale analysis”. In: *Environ. Res. Lett.* (2012). doi: <https://doi.org/10.1088/1748-9326/7/1/014037>. 590
- [12] N.W. Arnell and B. Lloyd-Hughes. “The global-scale impacts of climate change on water resources and flooding under new climate and socio-economic scenarios”. In: *Climatic Change* (2014). doi: <https://doi.org/10.1007/s10584-013-0948-4>. 591
- [13] Mohammad Reza Alizadeh, Jan Adamowski, Mohammad Reza Nikoo, Amir AghaKouchak, Philip Dennison, and Mojtaba Sadegh. “A century of observations reveals increasing likelihood of continental-scale compound dry-hot extremes”. In: *Science advances* (2020). doi: <https://doi.org/10.1126/sciadv.aaz4571>. 592
- [14] Hervé Douville, Krishnan Raghavan, James Renwick, Richard P Allan, Paola A Arias, Mathew Barlow, Ruth Cerezo-Mota, Annalisa Cherchi, Thian Y Gan, Joëlle Gergis, et al. “Water cycle changes”. In: (2021). 593
- [15] Fuad Yassin, Saman Razavi, Mohamed Elshamy, Bruce Davison, Gonzalo Sapriza-Azuri, and Howard Wheeler. “Representation and improved parameterization of reservoir operation in hydrological and land-surface models”. In: *Hydrology and Earth System Sciences* (2019). doi: <https://doi.org/10.5194/hess-23-3735-2019>. 594
- [16] Inne Vanderkelen, Shervan Gharari, Naoki Mizukami, Martyn P Clark, David M Lawrence, Sean Swenson, Yadu Pokhrel, Naota Hanasaki, Ann Van Griensven, and Wim Thiery. “Evaluating a reservoir parametrisation in the vector-based global routing model mizuRoute (v2.0.1) for Earth system model coupling”. In: *Geoscientific Model Development Discussions 2022* (2022). doi: <https://doi.org/10.5194/gmd-15-4163-2022>. 595

580
581
582
583
584
585
586
587
588
589
590
591
592
593
594
595
596
597
598
599
600
601
602
603
604
605
606
607
608
609
610
611
612
613
614
615
616
617
618
619
620
621
622
623
624
625
626
627
628

- [17] Edwin H Sutanudjaja, Rens Van Beek, Niko Wanders, Yoshihide Wada, Joyce HC Bosmans, Niels Drost, Ruud J Van Der Ent, Inge EM De Graaf, Jannis M Hoch, Kor De Jong, et al. “PCR-GLOBWB 2: a 5 arcmin global hydrological and water resources model”. In: *Geoscientific Model Development* (2018). doi: <https://doi.org/10.5194/gmd-11-2429-2018>. 629-632
- [18] Naota Hanasaki, Sayaka Yoshikawa, Yadu Pokhrel, and Shinjiro Kanae. “A global hydrological simulation to specify the sources of water used by humans”. In: *Hydrology and Earth System Sciences* (2018). doi: <https://doi.org/10.5194/hess-22-789-2018>. 633-635
- [19] Peter Burek, Yusuke Satoh, Taher Kahil, Ting Tang, Peter Greve, Mikhail Smilovic, Luca Guil-laumot, and Yoshihide Wada. “Development of the Community Water Model (CWatM v1. 04) A high-resolution hydrological model for global and regional assessment of integrated water resources management”. In: (2019). doi: <https://doi.org/10.5194/gmd-13-3267-2020>. 636-639
- [20] Bram Droppers, Wietse HP Franssen, Michelle TH Van Vliet, Bart Nijssen, and Fulco Ludwig. “Simulating human impacts on global water resources using VIC-5”. In: *Geoscientific Model Development Discussions* (2020). doi: <https://doi.org/10.5194/gmd-13-5029-2020>. 640-642
- [21] Hannes Müller Schmied, Denise Cáceres, Stephanie Eisner, Martina Flörke, Claudia Herbert, Christoph Niemann, Thedini Asali Peiris, Eklavya Popat, Felix Theodor Portmann, Robert Reinecke, et al. “The global water resources and use model WaterGAP v2. 2d: Model descrip-tion and evaluation”. In: *Geoscientific Model Development* (2021). doi: <https://doi.org/10.5194/gmd-14-1037-2021>. 643-647
- [22] Sabin I Taranu, David M Lawrence, Yoshihide Wada, Ting Tang, Erik Kluzek, Sam Rabin, Yi Yao, Steven J De Hertog, Inne Vanderkelen, and Wim Thiery. “Bridging the gap: a new module for human water use in the Community Earth System Model version 2.2. 1”. In: *EGU sphere 2024* (2024). doi: <https://doi.org/10.5194/egusphere-2024-362>. 648-651
- [23] Maryna Stokal, Carolien Kroeze, Mengru Wang, Zhaohai Bai, and Lin Ma. “The MARINA model (Model to Assess River Inputs of Nutrients to seAs): Model description and results for China”. In: *Science of the Total Environment* (2016). doi: <https://doi.org/10.1016/j.scitotenv.2016.04.071>. 652-655
- [24] Edward R Jones, Marc FP Bierkens, Niko Wanders, Edwin H Sutanudjaja, Ludovicus PH Van Beek, and Michelle TH Van Vliet. “DynQual v1. 0: a high-resolution global surface water qual-ity model”. In: *Geoscientific Model Development Discussions* (2023). doi: <https://doi.org/10.5194/gmd-16-4481-2023>. 656-659
- [25] Naota Hanasaki, Sayaka Yoshikawa, Kaoru Kakinuma, and Shinjiro Kanae. “A seawater de-salination scheme for global hydrological models”. In: *Hydrology and Earth System Sciences* (2016). doi: <https://doi.org/10.5194/hess-20-4143-2016>. 660-662
- [26] TIE Veldkamp, Y Wada, JCJH Aerts, P Döll, Simon N Gosling, J Liu, Y Masaki, T Oki, Se-bastian Ostberg, Y Pokhrel, et al. “Water scarcity hotspots travel downstream due to human interventions in the 20th and 21st century”. In: *Nature communications* (2017). doi: <https://doi.org/10.1038/ncomms15697>. 663-666
- [27] Zhongwei Huang, Xing Yuan, and Xingcai Liu. “The key drivers for the changes in global water scarcity: Water withdrawal versus water availability”. In: *Journal of Hydrology* (2021). doi: <https://doi.org/10.1016/j.jhydrol.2021.126658>. 667-669
- [28] Xingcai Liu, Wenfeng Liu, Liu Liu, Qihong Tang, Junguo Liu, and Hong Yang. “Environmental flow requirements largely reshape global surface water scarcity assessment”. In: *Environmental Research Letters* (2021). doi: <https://doi.org/10.1088/1748-9326/ac27cb>. 670-672
- [29] Yusuke Satoh, Taher Kahil, Edward Byers, Peter Burek, Günther Fischer, Sylvia Tramberend, Peter Greve, Martina Flörke, Stephanie Eisner, Naota Hanasaki, et al. “Multi-model and multi-scenario assessments of Asian water futures: The Water Futures and Solutions (WFaS) initia-tive”. In: *Earth’s Future* (2017). doi: <https://doi.org/10.1002/2016EF000503>. 673-675

629
630
631
632
633
634
635
636
637
638
639
640
641
642
643
644
645
646
647
648
649
650
651
652
653
654
655
656
657
658
659
660
661
662
663
664
665
666
667
668
669
670
671
672
673
674
675
676

- [30] Venla Niva, Jialiang Cai, Maija Taka, Matti Kummu, and Olli Varis. “China’s sustainable water-energy-food nexus by 2030: Impacts of urbanization on sectoral water demand”. In: *Journal of Cleaner Production* (2020). doi: <https://doi.org/10.1016/j.jclepro.2019.119755>. 677
- [31] Edward Byers, Matthew Gidden, David Leclère, Juraj Balkovic, Peter Burek, Kristie Ebi, Peter Greve, David Grey, Petr Havlik, Astrid Hillers, et al. “Global exposure and vulnerability to multi-sector development and climate change hotspots”. In: *Environmental Research Letters* (2018). doi: <https://doi.org/10.1088/1748-9326/aabf45>. 678
- [32] Yuanyuan Yin, Lei Wang, Zhongjing Wang, QiuHong Tang, Shilong Piao, Deliang Chen, Jun Xia, Tobias Conradt, Junguo Liu, Yoshihide Wada, et al. “Quantifying water scarcity in northern China within the context of climatic and societal changes and south-to-north water diversion”. In: *Earth’s Future* (2020). doi: <https://doi.org/10.1029/2020EF001492>. 679
- [33] Daniel Viviroli, Matti Kummu, Michel Meybeck, Marko Kallio, and Yoshihide Wada. “Increasing dependence of lowland populations on mountain water resources”. In: *Nature Sustainability* (2020). doi: <https://doi.org/10.1038/s41893-020-0559-9>. 680
- [34] Zhongwei Huang, Xingcai Liu, Siao Sun, Yin Tang, Xing Yuan, and QiuHong Tang. “Global assessment of future sectoral water scarcity under adaptive inner-basin water allocation measures”. In: *Science of the Total Environment* (2021). doi: <https://doi.org/10.1016/j.scitotenv.2021.146973>. 681
- [35] Ted Isis Elize Veldkamp, Fang Zhao, Philip J Ward, H De Moel, Jeroen CJH Aerts, H Müller Schmied, Felix T Portmann, Yoshimitsu Masaki, Yadu Pokhrel, Xingcai Liu, et al. “Human impact parameterizations in global hydrological models improve estimates of monthly discharges and hydrological extremes: a multi-model validation study”. In: *Environmental Research Letters* (2018). doi: <https://doi.org/10.1088/1748-9326/aab96f>. 682
- [36] Feng Zhou, Yan Bo, Philippe Ciais, Patrice Dumas, QiuHong Tang, Xuhui Wang, Junguo Liu, Chunmiao Zheng, Jan Polcher, Zun Yin, et al. “Deceleration of China’s human water use and its key drivers”. In: *Proceedings of the national academy of sciences* (2020). doi: <https://doi.org/10.1073/pnas.1909902117>. 683
- [37] Zhongwei Huang, Mohamad Hejazi, Xinya Li, QiuHong Tang, Chris Vernon, Guoyong Leng, Yaling Liu, Petra Döll, Stephanie Eisner, Dieter Gerten, et al. “Reconstruction of global gridded monthly sectoral water withdrawals for 1971–2010 and analysis of their spatiotemporal patterns”. In: *Hydrology and Earth System Sciences* (2018). doi: <https://doi.org/10.5194/hess-22-2117-2018>. 684
- [38] Yaling Liu, Mohamad Hejazi, Page Kyle, Son H Kim, Evan Davies, Diego G Miralles, Adriaan J Teuling, Yujie He, and Dev Niyogi. “Global and regional evaluation of energy for water”. In: *Environmental Science & Technology* (2016). doi: <https://doi.org/10.1021/acs.est.6b01065>. 685
- [39] Mohamad I Hejazi, J Edmonds, L Clarke, P Kyle, Evan Davies, Vaibhav Chaturvedi, M Wise, P Patel, Jiyong Eom, and K Calvin. “Integrated assessment of global water scarcity over the 21st century under multiple climate change mitigation policies”. In: *Hydrology and Earth System Sciences* (2014). doi: <https://doi.org/10.5194/hess-18-2859-2014>. 686
- [40] Yoshihide Wada, LPH Van Beek, Daniel Viviroli, Hans H Dürr, Rolf Weingartner, and Marc FP Bierkens. “Global monthly water stress: 2. Water demand and severity of water stress”. In: *Water Resources Research* (2011). doi: <https://doi.org/10.1029/2010WR009791>. 687
- [41] Nathalie Voisin, Lu Liu, Maryam Hejazi, T Tesfa, Hongyi Li, Maoyi Huang, Ying Liu, and LR Leung. “One-way coupling of an integrated assessment model and a water resources model: evaluation and implications of future changes over the US Midwest”. In: *Hydrology and Earth System Sciences* (2013). doi: <https://doi.org/10.5194/hess-17-4555-2013>. 688
- [42] Mohamad I Hejazi, Nathalie Voisin, Lu Liu, Lisa M Bramer, Daniel C Fortin, John E Hathaway, Maoyi Huang, Page Kyle, L Ruby Leung, Hong-Yi Li, et al. “21st century United States emissions mitigation could increase water stress more than the climate change it is mitigating”. 689
- 690
- 691
- 692
- 693
- 694
- 695
- 696
- 697
- 698
- 699
- 700
- 701
- 702
- 703
- 704
- 705
- 706
- 707
- 708
- 709
- 710
- 711
- 712
- 713
- 714
- 715
- 716
- 717
- 718
- 719
- 720
- 721
- 722
- 723
- 724
- 725

- In: *Proceedings of the National Academy of Sciences* (2015). DOI: <https://doi.org/10.1073/pnas.1421675112>. 726
727
- [43] Ianna Raissa Moreira Dantas, Ruth Delzeit, and Gernot Klepper. “Economic research on the global allocation of scarce Water resources needs better data”. In: *Water Economics and Policy* (2021). DOI: <https://doi.org/10.1142/S2382624X21500132>. 728
729
730
- [44] Zarrar Khan, Isaac Thompson, Chris R Vernon, Neal T Graham, Thomas B Wild, and Min Chen. “Global monthly sectoral water use for 2010–2100 at 0.5° resolution across alternative futures”. In: *Scientific Data* (2023). DOI: <https://doi.org/10.1038/s41597-023-02086-2>. 731
732
733
- [45] Detlef P Van Vuuren, Jae Edmonds, Mikiko Kainuma, Keywan Riahi, Allison Thomson, Kathy Hibbard, George C Hurtt, Tom Kram, Volker Krey, Jean-Francois Lamarque, et al. “The representative concentration pathways: an overview”. In: *Climatic change* (2011). DOI: <https://doi.org/10.1007/s10584-011-0148-z>. 734
735
736
737
- [46] Brian C O’Neill, Elmar Kriegler, Kristie L Ebi, Eric Kemp-Benedict, Keywan Riahi, Dale S Rothman, Bas J Van Ruijven, Detlef P Van Vuuren, Joern Birkmann, Kasper Kok, et al. “The roads ahead: Narratives for shared socioeconomic pathways describing world futures in the 21st century”. In: *Global environmental change* (2017). DOI: <https://doi.org/10.1016/j.gloenvcha.2015.01.004>. 738
739
740
741
742
- [47] Katja Frieler, Stefan Lange, Franziska Piontek, Christopher PO Reyer, Jacob Schewe, Lila Warszawski, Fang Zhao, Louise Chini, Sebastien Denvil, Kerry Emanuel, et al. “Assessing the impacts of 1.5 C global warming—simulation protocol of the Inter-Sectoral Impact Model Intercomparison Project (ISIMIP2b)”. In: *Geoscientific Model Development* (2017). DOI: <https://doi.org/10.5194/gmd-10-4321-2017>. 743
744
745
746
747
- [48] Neal T Graham, Mohamad I Hejazi, Min Chen, Evan GR Davies, James A Edmonds, Son H Kim, Sean WD Turner, Xinya Li, Chris R Vernon, Katherine Calvin, et al. “Humans drive future water scarcity changes across all Shared Socioeconomic Pathways”. In: *Environmental Research Letters* (2020). DOI: <https://doi.org/10.1088/1748-9326/ab639b>. 748
749
750
751
- [49] William Wint, Timothy Robinson, et al. “Gridded livestock of the world 2007”. In: (2007). 752
- [50] Mohamad Hejazi, James Edmonds, Leon Clarke, Page Kyle, Evan Davies, Vaibhav Chaturvedi, Marshall Wise, Pralit Patel, Jiyong Eom, Katherine Calvin, et al. “Long-term global water projections using six socioeconomic scenarios in an integrated assessment modeling framework”. In: *Technological Forecasting and Social Change* (2014). DOI: <https://doi.org/10.1016/j.techfore.2013.05.006>. 753
754
755
756
757
- [51] Min Chen, Chris R Vernon, Neal T Graham, Mohamad Hejazi, Maoyi Huang, Yanyan Cheng, and Katherine Calvin. “Global land use for 2015–2100 at 0.05 resolution under diverse socioeconomic and climate scenarios”. In: *Scientific Data* (2020). DOI: <https://doi.org/10.1038/s41597-020-00669-x>. 758
759
760
761